NASA TECHNICAL NOTE

NASA TN D-6016

NASA TN D-6016

A SIMULATOR STUDY OF THE CONTROL OF LUNAR FLYING PLATFORMS BY PILOT BODY MOTIONS

by Paul R. Hill and David F. Thomas, Jr.

Langley Research Center
Hampton, Va. 23365

NATIONAL AERONAUTICS AND SPACE ADMINISTRATION • WASHINGTON, D. C. • DECEMBER 1970

1. Report No.	2. Government Accession No.	3. Recipient's Catalog No.
NASA TN D-6016		

4. Title and Subtitle	5. Report Date
A SIMULATOR STUDY OF THE CONTROL OF LUNAR FLYING PLATFORMS BY PILOT BODY MOTIONS	December 1970
	6. Performing Organization Code
7. Author(s)	8. Performing Organization Report No.
Paul R. Hill and David F. Thomas, Jr.	L-7304
	10. Work Unit No.
9. Performing Organization Name and Address	127-51-41-05
NASA Langley Research Center Hampton, Va. 23365	11. Contract or Grant No.
	13. Type of Report and Period Covered
12. Sponsoring Agency Name and Address	Technical Note
National Aeronautics and Space Administration Washington, D.C. 20546	14. Sponsoring Agency Code

15. Supplementary Notes

16. Abstract

This paper presents the results of an investigation of body-motion control of lunar-flying-platform configurations utilizing shirt-sleeved operators and a simulator with five degrees of freedom. The results show that lunar vehicles with moments of inertia up to 100 slug-ft^2 (136 kg-m^2) in pitch and 300 or 400 slug-ft^2 (407 or 542 kg-m^2) in roll should have satisfactory control qualities. The separation of the vehicle operator and thrust jets from the high-inertia vehicle elements by means of a low-inertia auxiliary platform resulted in satisfactory control in both pitch and roll over the range of equivalent lunar moments of inertia of 33 to 400 slug-ft^2 (45 to 542 kg-m^2). A description of a number of useful variations of body-motion control is presented.

17. Key Words (Suggested by Author(s))	18. Distribution Statement
Lunar transport vehicle Body-motion control Flying platform handling qualities Auxiliary platform control	Unclassified – Unlimited

19. Security Classif. (of this report)	20. Security Classif. (of this page)	21. No. of Pages	22. Price*
Unclassified	Unclassified	52	$3.00

*For sale by the National Technical Information Service, Springfield, Virginia 22151

A SIMULATOR STUDY OF THE CONTROL OF LUNAR FLYING PLATFORMS BY PILOT BODY MOTIONS

By Paul R. Hill and David F. Thomas, Jr.
Langley Research Center

SUMMARY

This paper presents the results of an exploratory investigation of body-motion control of lunar-flying-platform configurations utilizing shirt-sleeved operators and a simulator with five degrees of freedom. The results indicated that the natural-reflex-control concept has a valid application to the design of lunar flying vehicles at the moment of inertias of the test. The control concept was evaluated by means of pilot rating for a simulated task of moving a lunar vehicle from point to point at low speed and altitude. These ratings varied from satisfactory to unsatisfactory as the moments of inertia in pitch were increased from low to high values. Decreases in roll controllability with increasing inertia were much less pronounced. The isolation of the operator and thrust jets from the high-inertia airframe by means of an auxiliary control platform resulted in satisfactory simulations of pitch and roll control at all inertias of the test and a general improvement in controllability over the basic all-rigid configurations. This improvement is attributed to the low moment of inertia of the auxiliary platform and the rapid response to a control input which permitted the operator to prejudge and execute maneuvers more accurately.

Analyses of body-motion control of flying-platform-type vehicles is given along with mathematical solutions for simple cases. A description of a number of useful variations of body-motion control is presented.

INTRODUCTION

Lunar flying vehicles are under consideration for facilitating lunar exploration. However, the best method of controlling a lunar flying vehicle is in doubt. There are three commonly considered methods for controlling pitch and roll: the thrust-vector control method, the method of auxiliary thrusters, and the method utilizing the body motion of a standing man, which is sometimes referred to as natural-reflex or kinesthetic control. In thrust-vector control, the thrust axis is moved relative to the vehicle center of gravity. In body-motion control, the center of gravity is moved relative to a fixed thrust axis. Auxiliary thrusters are located to provide appropriate control couples. The use of body-motion control could simplify the design, lower the weight, and improve the reliability of

the vehicle by the elimination of either engine pivots or auxiliary rockets, pitch- and roll-control hardware, and possibly stability augmentation in pitch and roll.

Although it has been generally accepted that natural-reflex balancing is satisfactory at low values of moment of inertia, available evidence indicates a deterioration of handling qualities at increasing moments of inertia. However, past simulation studies of the effect of high moment of inertia on control by body motion (or weight shifting) have tended to be of poor quality because of the difficulty of simulation in a one earth gravity field. The principal approach to simulation of control by body motion has been by free flight in earth gravity. That this approach does not give a valid lunar simulation can be seen from the analyses presented in the appendix of this report which show that for equal vehicle control attitudes, the horizontal accelerations and distances traveled are six times greater in earth flight than in lunar flight and result in completely different control feedbacks to the pilot.

In order to get applicable data, a five-degree-of-freedom lunar flying platform simulator was developed at the Langley Research Center. (See ref. 1.) This simulator correctly simulated linear as well as angular motions. Initially, a number of limitations were present in this simulation, for example, the lack of a throttle, the lack of yaw control, the lack of vertical motion, the limited floor area which permitted a linear run of only 10 feet (3.05 meters), and a visual field different from the lunar environment. In an effort to reduce these limitations for the present research program, a much larger plastic floor was built. A dummy rate-of-climb control connected through an analog computer to an altimeter permitted a vertical profile to be simulated during a run between one point and another. A yaw control was also added. These controls gave the pilot a complement of duties which is considered to be important in the simulation. He controlled pitch and roll with body motion, and yaw and rate of climb with his hands, and was required to watch the altimeter while coordinating his simulated altitude with his horizontal position. The visual field was believed to be adequate for this exploratory type of investigation.

Since the handling qualities in this and virtually all other simulations were observed to deteriorate with increasing inertia, it was decided to simulate a lunar flying platform which had the rockets connected to an auxiliary, swiveling, low-inertia platform controlled by the feet. This idea was first utilized in reference 2.

The present test program resulted in comparative handling quality ratings for shirt-sleeve conditions over a range of inertia from 100 to 900 slug-ft^2 (136 to 1220 kg-m^2) without the man for both the basic and the revised vehicle with the low-inertia auxiliary control platform. A combination of unequal inertias, 300 slug-ft^2 (407 kg-m^2) about the pitch axis and 1200 slug-ft^2 (1627 kg-m^2) about the roll axis, was also tested. Other variables such as pilot vertical location relative to the simulator center of gravity and the effect of the added weight of a backpack were investigated.

SYMBOLS

a	acceleration
d_m	distance of operator's center of gravity from combined center of gravity of lunar vehicle
d_o	offset of operator's center of gravity above simulator center of curvature
d_v	distance of vehicle's center of gravity from combined center of gravity of lunar vehicle
e_m	linear displacement of operator's center of gravity from line of thrust for lunar vehicle or simulator
$F_{i,a}$	inertial force of auxiliary platform
$F_{i,b}$	inertial force due to ballast
$F_{i,d}$	inertial force due to air-pad dolly
$F_{i,m}$	inertial force of operator
g_e	acceleration of gravity constant, earth
I	moment of inertia
$K_{d,v}$	damping constant for lunar vehicle
$K_{d,s}$	damping constant for simulator
$K_{s,v}$	spring constant for lunar vehicle
$K_{s,s}$	spring constant for simulator
l	distance of simulator ballast weight from center of curvature
l_a	distance from pivot point to center of gravity of auxiliary platform

l_b distance from pivot point to center of gravity of ballast weight for simulator

l_f distance from pivot point to center of gravity of main frame

l_m distance from intersection of stand-on platform and line of thrust to center of gravity of operator

l_p distance from pivot point to surface of stand-on platform

M total mass

P period of oscillation

Q moment used in analysis of oscillation

Q_v moment acting on basic configuration of lunar vehicle

Q_s moment acting on basic configuration of simulator

$Q_{a,s}$ moment acting on auxiliary platform of simulator

$Q_{a,v}$ moment acting on auxiliary platform of lunar vehicle

$Q_{f,s}$ moment acting on main frame of simulator

$Q_{f,v}$ moment acting on main frame of lunar vehicle

R radius of spherical segment of simulator

T thrust

T_s thrust of simulator

T_v thrust of lunar vehicle

t time

W weight

W_a earth weight of auxiliary platform

W_b earth weight of ballast for simulator

W_d earth weight of air-pad dolly for simulator

W_e effective weight of man on lunar flying platform or on earth simulator

W_f earth weight of main frame of auxiliary platform configuration

W_m earth weight of operator

x horizontal displacement in plane of angular rotation for control analysis

$\dot{x}$ horizontal velocity in plane of angular rotation for control analysis

$\ddot{x}$ horizontal acceleration in plane of angular rotation for control analysis

β angular displacement of center line of main frame with respect to local vertical

γ angular displacement of thrust axis (that is, perpendicular to auxiliary platform) with respect to center line of main frame

δ angular displacement of the operator's center of gravity from the line of thrust measured about intersection of stand-on platform and line of thrust

θ angular displacement of thrust axis from local vertical

ω frequency of control oscillation

Subscripts:

a auxiliary platform

b ballast

d air-pad dolly

f	main frame
i	inertia
m	operator
max	maximum
p	auxiliary platform surface
s	simulator
t	total
v	lunar vehicle

Dots over symbols denote derivatives with respect to time.

BODY-MOTION CONTROL TECHNIQUES

The Task

Two types of control tasks are to be accomplished. One is to stabilize attitude as in hovering or cruising. This task is to observe small errors in vehicle attitude or attitude rate and apply moments to nullify the errors. The other task is to change attitude, as for accelerating the vehicle to a desired horizontal speed. This change in attitude involves leaning the body relative to the thrust vector in the desired direction of acceleration which puts in a control moment Q. Leaning the body gradually increases Q as a ramp function. The initiation of a horizontal acceleration by a variation of Q and the attitude and attitude rates, θ and $\dot{\theta}$, as a function of time might typically appear as in sketch (a). The control moment is typically held constant for a short period of time and

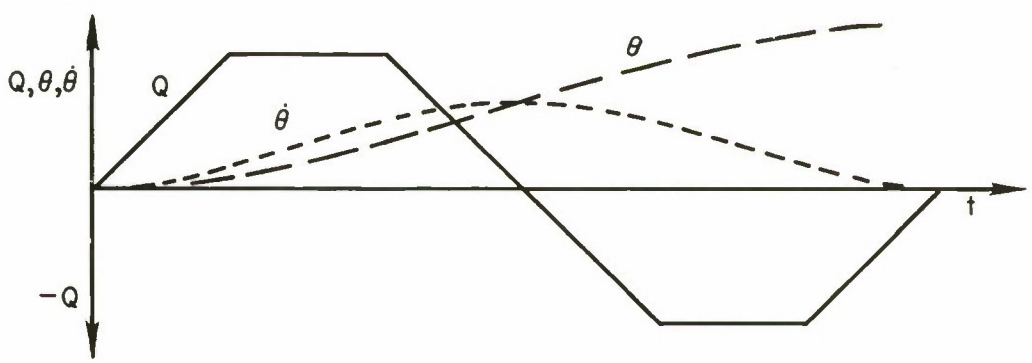

Sketch (a)

brought back to zero by the time $\dot{\theta}$ is maximum and θ has achieved half its value. An equal negative control effort is then required to reduce $\dot{\theta}$ to zero at the desired angle. The control process must be reversed to stop the horizontal acceleration.

Natural-Reflex Control

The control of a flying vehicle by natural reflexes was described in reference 3 by its inventor Charles Zimmerman, who realized that a person standing or balancing himself on a flying platform would by natural-reflex actions apply moments in the proper sense to balance the platform. Assume that a man is standing on a platform the lift of which can be represented by a thrust vector (fig. 1) and that this man senses that he is falling forward, perhaps because the machine is beginning to tilt forward (fig. 1(a)). He will automatically press down with his toes which will stop his body's undesired forward pitching and rotate his body backward, or upright, as shown by the dashed lines. This action alone can place his body center of gravity behind the thrust axis, by the angle θ_V, and creates a moment to right the machine which is proportional to the distance from the man's center of mass to the thrust axis, $l_m \sin \theta_V$. Such a pressing down with the toes can be physically accomplished by an angle torque which is transmitted to the platform as a positive pitching moment. This torque momentarily tends to rotate the platform forward. Although this feature is not desirable, the end result is that the thrust vector is tilted farther forward of the man's center of gravity and thus creates a negative moment which rotates the platform to the upright position. If the man sensed that he was tilting backward, he would reduce the pressure on the balls of his feet and the reverse process would occur. If the body is leaned laterally, similar results are obtained. Thus, the man in balancing himself can stabilize the platform.

This description of natural-reflex balancing was the status of the understanding of this method of balancing at the time that reference 3 was published. However, the work of reference 2 (1954) contributed a significant advance to the art and understanding of natural-reflex balancing. "Body English" or bending the body at the waist gives an improved natural-balancing technique. This body motion or bending is accomplished by "leading" with the hips in any direction needed for balance or control accompanied by an almost imperceptible counter-bending at the waist. This form of control also permits the operator to be more relaxed than in the equivalent rigid-body leaning technique. The reason it works so smoothly is that at initiation, the moment of inertia of the hips and waist about the feet is bucked against the moment of inertia of the head, chest, and shoulders (which is greater) and results in the greater displacement of the midbody in the appropriate direction to balance the vehicle. The initial adverse ankle moment input into the vehicle is thereby eliminated. This analysis explains why an attempt to analyze reflex control by treating the body as a rigid beam torqued at one end may give erroneous results.

A balancing body is not rigid. A light handhold on the rails or controls is useful to provide damping, to steady the body, and to prevent small oscillations.

A pilot or operator can exert greater input or control moments laterally about the roll axis than about the pitch axis because the natural spread-foot stance permits a greater lateral than forward-and-aft shift of body weight. Control about the roll axis is usually very smooth; leading with the hips for roll control consists of moving the torso on the parallelogram or trapezoid having the ankle joints and hip joints as vertices.

Manual assist.- Because a man's feet are only about a foot (0.305 meter) long, fore or aft control-moment inputs without manual assist are limited to his weight times about 1/2 foot (0.152 meter). To increase the control input he can exert in pitch requires supporting his body by some form of handhold while he leans farther than would otherwise be possible. Such a manual assist is usually applied gently but with a firmer handhold than with the damping function described above.

One form of manual assist herein referred to as the impulsive technique was developed for obtaining rapid response with high-inertia configurations. This technique consists of imparting large impulsive control moments to the vehicle structure as follows: For positive angular control velocities, a forward lunge by the operator was suddenly arrested by the hands pushing on the vertical rails. Conversely, a negative control input was obtained by leaning backward and jerking on the vehicle frame. It was observed that this technique produced nearly instantaneous changes in angular velocity. This method was used only when the operator wished to move a high-inertia configuration about rapidly.

Application.- The most effective or preferred variation of body-motion control depends on vehicle moment of inertia and on whether the vehicle has a low-inertia platform. The dependence of the preferred variation on vehicle parameters is discussed in the section "Results and Discussion."

DESCRIPTION OF SIMULATOR

General Description of Flight Vehicle

The basic configuration of the lunar vehicle being simulated consists of a generous platform for the man to stand and walk on, supported on the lunar surface by landing legs and in flight by one or two rockets with thrust alined to pass through the center of gravity of the vehicle as well as near the center of the platform. (See fig. 1(a).) The upper framework consists of two or four vertical rails for handholds laid out in a square as large as the platform. The two forward rails support the instrument and control panel which, in turn, may support the rate-of-climb and yaw controls. The yaw system design is quite flexible. The type simulated was the auxiliary thruster variety with two small motors placed to give a positive yawing couple and two to give a negative couple. By

shifting his body weight in a manner described under "Body-Motion Control Techniques," the pilot induces pitch and roll which, in turn, result in the desired translations. The dynamic stability of this fixed-jet flying platform is neutral.

General Description of Simulator

A simulation of the lunar flying platform requires that the angular accelerations and linear accelerations be equal to those of the lunar vehicle and that it have neutral dynamic stability. The spherical-segment or roly-poly simulator described below meets these requirements.

In the basic configuration, the stand-on platform, hereafter referred to as the platform, was rigidly mounted to a spherical segment which permitted motion in pitch and roll. (See figs. 1(b), 2, and 3.) The mounting of the auxiliary platform to the spherical segment is described later. The spherical segment rested on a flat plate which was mounted on an air-pad dolly. The air-pad dolly was free to translate over a smooth, level, epoxy floor surface. In order to obtain a high range of moment of inertia, four lightweight, truss-type booms, clearly visible in figure 2, were attached to move with the platform and spherical segment in pitch, roll, and yaw. Moments of inertia were varied by attaching lead weights to the boom tips in 20-pound (9.1-kg) increments, and for the lowest inertia the booms were removed. A tilt restraint ring was used (fig. 3) to limit the tilt of the simulator to $\pm 13^{\circ}$.

To obtain translation, a pair of air jets were attached to the booms. The jet reaction lifted about one-sixth of the combined weight of the man and simulator. The other five-sixths of the weight was supported by the air pads on the floor. Horizontal accelerations and velocities equal to lunar values were obtained from the horizontal components of thrust.

Air to the simulator main jets and yaw control came through flexible hoses supported on the floor by air pads. The air pressure was controlled from a position adjacent to the 40- by 45-foot (12.2- by 13.7-meter) epoxy floor and was not under the direct control of the operator.

Satisfying the angular acceleration criteria requires larger moments of inertia for the simulator than for the flight vehicle. The ratio is discussed under "Analysis." Symmetrical moments of inertia (equal in pitch and roll) of 100, 300, 600, and 900 slug-ft^2 (136, 407, 813, and 1220 kg-m^2) were employed for most of the tests. For a standard man of 166.4 pounds (740.15 newtons), these moments of inertia correspond to control sensitivities of 7.95, 2.65, 1.33, and 0.88 (deg/sec^2)/inch (0.313, 0.104, 0.052, and 0.035 (deg/sec^2)/mm) displacement of the center of mass of the operator from the neutral position. An unsymmetrical inertia configuration of 300 slug-ft^2 (407 kg-m^2) in pitch and

1200 slug-ft^2 (1627 kg-m^2) in roll represented a flying platform with propellant tanks located on the pitch axis on either side of the platform.

Auxiliary Platform Configuration

The auxiliary platform design differed from the basic design in that the jets were coupled with the low-inertia auxiliary platform by means of the tubular booms on which they were mounted. In this manner the jets were decoupled from the high-inertia main frame and thus the operator could rapidly reorient the platform and jets. The auxiliary platform would also perform a useful function in landing or take-off from an inclined surface since the jets can be oriented vertically while the landing gear conforms to the terrain, as shown in figure 4. Figure 5 is a photograph showing the auxiliary platform design. The auxiliary platform was attached to the spherical segment by the use of a universal joint with its pivot point just below the surface of the platform. The jets were alined so that the resultant thrust was normal to the auxiliary platform. The direction of the resultant thrust was thus affected by both the tilt angle of the main frame and the angle of the auxiliary platform relative to the main frame. The moment of inertia of the platform and tubular frame were approximately 14 slug-ft^2 (19 kg-m^2) about the pitch and roll axes. The control sensitivities were approximately 19 (deg/sec^2)/inch (0.748 (deg/sec^2)/mm) of operator displacement from the neutral position in pitch and roll. This control sensitivity value did not include the effect of the dashpot and spring restraints, but was the value at the first instant of deflection.

Initial trials with the pivoted auxiliary platform indicated the need for some sort of restraint between the auxiliary platform and the high-moment-of-inertia elements of the simulator to eliminate oscillations in the stand-on platform. The system finally adopted was parallel installations of springs and dashpots about the pitch and roll axes. The springs provided 5.67 ft-lb (7.59 m-N) restoring moment per degree of auxiliary platform tilt, and the near-optimum dashpots provided a damping coefficient of $\frac{4.60 \text{ ft-lb}}{\text{deg/sec}}$ $\left(\frac{6.24 \text{ m-N}}{\text{deg/sec}}\right)$ for $I = 100$ slug-ft^2 (136 kg-m^2) and $\frac{1.90 \text{ ft-lb}}{\text{deg/sec}}$ $\left(\frac{2.58 \text{ m-N}}{\text{deg/sec}}\right)$ for values of I from 300 to 900 slug-ft^2 (407 to 1220 kg-m^2). When the auxiliary platform is chocked with blocks, it becomes the basic configuration. (See fig. 6.)

Variations in Platform Height

Variations in platform height with respect to the center of curvature of the spherical surface were provided for the basic configuration only, by removable stools 1/2 foot and 1 foot (0.152 meter and 0.305 meter) in height placed on the locked auxiliary platform, as shown in figure 7. The center of gravity of the operator ranged from approximately

1/2 to 1.5 feet (0.152 to 0.46 meter) above the center of curvature of the spherical surface by using one or both stools.

Manual Controls

The yaw control consisted of a lever-actuated two-way air valve located at the bottom center of a control panel in front of the operator. (See fig. 8.) The valve was connected to two pairs of air jets located on opposite booms and directed so that when a pair of jets were activated, a positive or negative yawing couple was introduced. The valve had a spring return to the neutral or off position.

In order to load the operator with tasks to accomplish while performing a translation maneuver, a rate-of-climb control knob was mounted on the control panel and was connected through a computer located back of the control panel to an altitude indicator on the panel. (See fig. 8.) Since the simulator angles were small, the cosine function of the tilt angle was neglected by the computer. This choice of control implies the lunar vehicle being simulated had a computer-controlled throttle. Such a device would make flying easier but may not be needed.

The operator controlled an air-pad switch with which he turned on or off the blowers supplying air to the air pads. With this switch and his climb control, he could simulate a take-off.

ANALYSIS

Simulation

Any complete simulation of a lunar flying platform must duplicate all angular and linear motions. With a pilot in the loop, these motions must be duplicated in real time. This statement means that all the angular and linear acceleration responses to control inputs must be duplicated and, as a result, all velocity and displacement time histories are faithfully followed.

The problem encountered in an earth simulation is that earth gravity is six times lunar gravity. This difference would scarcely be a problem for an all-mechanical system, but with man in the control loop in an important way as in body-motion control, the problem arises that the forces of gravity on the man are six times too great and for a given body motion the control moments are higher than those on the moon. Also, with a jet-supported vehicle, an additional problem arises in that if the jet supports the full earth weight of the vehicle, the jet forces are six times too high and it follows that all linear accelerations, velocities, and distances will be six times too great.

The appendix of this paper is devoted to a mathematical discussion of the validity of the present method of simulating angular and linear motion time history for both the basic configuration and for the auxiliary platform control. The present discussion leaves the proofs to the appendix, but discusses the physical principles involved in the simulation.

The problems mentioned make this a difficult simulation problem and no known method will be completely satisfactory. Several approaches are being considered. The best would surely be to carry a lightweight research flight vehicle to the moon. The most common attempted in the past is a free-flight vehicle in earth gravity. Here linear accelerations, velocities and distances are necessarily six times too great and the linear excursions due to vehicle oscillation resulting from control feedback have been found to be vicious and unrealistic. Two much more applicable methods may be considered. One is the method of supporting five-sixths of the weight of the vehicle by an overhead traveling suspension and five-sixths of the weight of the man by a separate suspension system. The vehicle then supports one-sixth of the man's weight and the vehicle jet propulsion one-sixth of the total weight. This method has advantages in that either an actual lunar flying platform or a mock-up can be tested because inertias do not need to be scaled. Other advantages are that all control forces and moments exerted by the pilot are true lunar values and six degrees of freedom can be simulated. There are almost no theoretical disadvantages to this system. The practical difficulty is that a great deal of painstaking work is required to design and develop the simulation, in particular, the suspensions. The other method is a simple method of intermediate excellence, the five-degree-of-freedom simulation described herein. Only minor development problems were encountered with this simulation.

In the present simulation, hovering thrust or any other applicable lunar thrust (up to a value approaching 6 lunar gravities) can be simulated. The thrust-mass ratio was not scaled. The thrust was held constant at values corresponding approximately to lunar hovering. The air-pad dolly and floor support the remainder of the weight. Except for minor restrictions such as air-pad friction and air-hose forces, linear accelerations corresponding to any jet-attitude angle are faithfully reproduced at lunar values. This reproduction of forces and accelerations has been found to be extremely important because of the accompanying feedback cues to the human balance mechanism. The duplication of angular accelerations is accomplished not by scaling down the control moments but by scaling up the moments of inertia. If equal body motions are assumed, the scaling ratio for equal angular acceleration is the ratio of earth weight to lunar apparent weight in flight

$$\frac{\text{Simulator moment of inertia}}{\text{Lunar vehicle moment of inertia}} = \frac{\text{Earth operator weight}}{\text{Lunar pilot mass} \times \text{Lunar acceleration}}$$

One would expect this ratio to be about six and it would be if the simulator operator were dressed in a pressure suit and backpack. However, for the present tests the simulator operators were in shirt sleeves. Since a suited astronaut with oxygen supply, and so forth, has his mass very close to being doubled, the scaling ratio for the present tests was taken as 3.

If the scaling ratio is 3, the absolute values of the control forces, put in by and felt by the simulator operator, are three times higher than is felt by the corresponding lunar pilot. The lunar pilot is working one-third as hard but gets the same results for a given body motion. The only question left open is, with lower absolute forces and work effort, are his motions the same? It should be borne in mind that the operator in any earth simulation will probably feel as heavy as usual. It is the man-vehicle interface forces that are greater in this simulation than in the suspension method. This effect and other simulation anomalies are discussed in the section on "Simulator Anomalies."

The auxiliary platform can be thought of as a foot-operated thrust-vector control system with a 1:1 coupling ratio. Inertias scale the same as in the basic configuration. Since all lunar moments must be reduced by the same ratio, the auxiliary platform spring constant and dashpot damping coefficients should be divided by the scaling ratio to obtain values for the equivalent lunar vehicle. The simulator and flight vehicle should have the same relative location of the rocket pivot point and vehicle center of gravity; thus, the jet thrusts would have the same moment arm. The platform pivot point is immaterial unless it happens to also be the rocket pivot point. To match the current tests, the rocket pivots would be about 3 feet (0.91 meter) below the vehicle center of gravity. If desired, the platform could be higher and connected by a linkage. With these provisions it is shown in the analysis of simulation laws in the appendix that the simulator will faithfully follow a given time history of control inputs.

Simulator Anomalies

The five-degree-of-freedom simulator provided an effective tool for the exploratory research program reported upon in this paper and was also useful as a demonstration vehicle; however, certain differences from the true lunar vehicle exist. These differences are:

(1) Visual cues are necessarily somewhat different on earth than on the moon; for example, being inside a building rather than over a lunar landscape, having no dust, and so forth. The lack of actual altitude may be the biggest input difference in visual cues but the effect of this difference is unknown. It was originally thought that increasing the floor size might affect pilot rating by reducing apprehension through more favorable visual cues. No such change was observed, probably because it was found that the operator took his translation cues from the floor in the immediate area below the simulator.

(2) The pilot ratings strictly apply to a task of moving the vehicle a short distance at low velocity at very low elevation. The correlation with other tasks is unknown.

(3) Some extraneous forces and moments are present in the system because of the following factors:

(a) The maximum floor slope of approximately 0.0001 had negligible effects.

(b) The air-bearing friction coefficient of about 0.001 was essentially negligible.

(c) Pressure hose forces and moments put in the greatest disturbances and slightly increased the difficulty of operating the simulator. These forces masked the effects of air-bearing friction and the moments caused the operator to activate yaw controls more frequently than would be the case in flight.

(4) Although horizontal acceleration is correct, the vertical acceleration field is six times too large. This difference has two side effects:

(a) The absolute values of the control forces which the operator feels and exerts are larger by the ratio of the scale factor than they would be on the moon. The operator is also accomplishing more work than the lunar pilot.

(b) The resultant acceleration field is oriented more vertically than is the case with a lunar flying platform where the acceleration field is always normal to the platform. Thus, the feel of the simulator to the operator is a little different at the larger angles of simulator inclination than would be the case for the lunar flying platform; the operator has some tendency to fall off the simulator which would not be the case on the flying platform. However, if the operator has a handhold on controls or on the frame, such a tendency is hardly noticed.

(5) The simulator had a $\pm 13^{o}$ angle limitation. However, most operators only used a maximum of about 10^{o}.

(6) The use of a rate control on indicated altitude made the altitude control task easier than would have been the case with an ordinary throttle which is an acceleration control and implies a rate control on the flight vehicle.

(7) The use of a pressurized space suit was beyond the scope of the present exploratory investigation. The possible restrictions of body motion and of vision imposed by a space suit may be serious and warrant investigation.

Oscillations

It is, of course, desirable to put in a control-moment sequence in pitch and roll which would deadbeat the vehicle angular motion to a desired new attitude. If the vehicle is overcontrolled and overshoots the desired attitude, and an overstrong negative input is made to bring the attitude back, an undesired rocking motion is initiated. The equations of motion for such a rocking motion with a sinusoidal forcing function and appropriate initial conditions are derived in the appendix. They apply both to free flight and to a simulation. The moment input Q and the initial conditions may be summarized as follows by using ω and t as angular frequency and time:

$$Q = Q_{max} \sin \omega t \tag{1}$$

with angle θ and displacement x equal to zero at t equal zero. (See appendix for conditions on $\dot{\theta}$ and $\dot{x}$.) From the appendix, the following solutions for attitude and position are obtained:

$$\theta = -\frac{Q_{max}}{I\omega^2} \sin \omega t \tag{2}$$

$$x = \frac{T}{M} \frac{Q_{max}}{I\omega^4} \sin \omega t \tag{3}$$

In the current series of experiments, T/M is set at or near 1/6 earth g or at about 5.4 ft/sec^2 (1.65 m/sec^2) and it can be seen from equation (3) that oscillatory displacements x are proportional to T/M and are smaller for a lunar flight where thrusts are reduced than for an earth flight. Equation (2) shows that the ratio of moment input to moment of inertia must be the same for the lunar vehicle and the simulator to give equal values of angle.

It is also shown in the appendix that if a pilot in free flight or a simulator operator holds his body at a fixed attitude in space and if either flight vehicle or simulator oscillations exist, the oscillations have a natural period much like those of a torsion pendulum. The period of such oscillations is treated in the appendix and in the section "Results and Discussion."

TEST PROCEDURES

Task and Techniques

The task generally performed consisted of a simulated flight from a point to another point 26 feet (7.92 meters) away while following a simulated flight profile as shown in figure 9. Starting with the simulator centered over a 6-foot-diameter (1.83-meter) circle

(painted on the floor), the operator opened the throttle and initiated an indicated climb rate of about 10 ft/sec (3.05 m/sec) and immediately raised a hand to signal that the test had begun. Upon noting an indicated altitude of about 10 feet (3.05 meters) or more, the operator tilted the foot platform toward the destination to initiate the horizontal motion. Upon achieving an altitude reading of 100 feet (≈30.50 meters), the climb rate was reduced to zero. About this time, or at halfway to the target at the latest, the positive acceleration was stopped by leveling the foot platform. Descent was generally initiated at about the midpoint of the run at a value of about 10 ft/sec (3.05 m/sec). Deceleration of horizontal speed was initiated whenever the operator desired but typically about 10 feet (3.05 meters) from the destination. Continued monitoring and adjustment of the descent rate was required as the operator strove to stop at the center of the target circle at the same time as touching down. In a variation of this technique, the operator hovered while centering the vehicle over the target and then descended. At this point a hand signal was given for the purpose of timing the run. Typical runs lasted 30 to 40 seconds. Throughout the run, the operator was fairly active at the yaw controller. All operators were right-handed, and when not adjusting the rate of climb or giving a timing signal, they generally held onto the yaw-control lever with the right hand, and gave inputs as desired.

The data taken were a pilot rating, the target miss distance, and the time to make the run.

Operational factors or features used for the rating included:

(a) Rocking of the simulator
(b) Over control or undercontrol of yaw
(c) Deviations from a smoothly accelerated and decelerated forward velocity (A severe case might involve a premature stop during final approach)
(d) Excessive hovering to center the machine in the target circle
(e) Observable miss distance
(f) The physical effort needed for control
(g) Coordination of all parts of the task

The pilot rating scale used is shown in table I. (It is essentially the original Cooper rating scale as given in ref. 4.) The parameters tested are given in table II.

Test data from the lunar flying platform simulator was obtained from five operators with code symbols, H, T, J, W, and R. Some of their characteristics and professional experience are given in table III.

RESULTS AND DISCUSSION

Results With Locked Auxiliary Platform

Normal platform elevation.- Figure 10 shows operator rating data based on handling qualities from runs made by operators H, J, T, R, and W with the platform locked; that is, from the spherical segment upward the simulator is rigid. Pilot ratings are given for various moments of inertia. The mean pilot rating varies from 2.5 at 100 slug-ft^2 (136 kg-m^2) to about 4.25 at 900 slug-ft^2 (1220 kg-m^2). The important result from the rating data is that a median pilot rating of from 2.5 at I = 100 slug-ft^2 (136 kg-m^2) to 2.8 at I = 300 slug-ft^2 (407 kg-m^2) was satisfactory, but the ratings of 3.75 and 4.25 at I = 600 slug-ft^2 and 900 slug-ft^2 (813 and 1220 kg-m^2), while possibly acceptable, are not satisfactory and indicate a need for improvement.

Experience with a variety of spacecraft indicates that handling quality deterioration with increasing inertia as in figure 10 is chargeable to the corresponding decrease in control sensitivity or angular acceleration in pitch and roll when a control input is made; that is, the high-inertia machine responds too slowly to a pitch or roll control input to satisfy the pilot. Miss distances are shown in table II and for the nontest pilot subjects vary from an average of 0.3 foot (0.09 meter) at 100 slug-ft^2 (136 kg-m^2) to an average of 0.75 foot (0.23 meter) at 900 slug-ft^2 (1220 kg-m^2). The test pilot subjects accepted miss distances on the order of 1.0 foot (0.30 meter) over the range of inertias tested; they concentrated more on bringing the altitude and translational velocities to zero simultaneously.

At inertias of 100 and 300 slug-ft^2 (136 and 407 kg-m^2), operators usually determined that an optimum flight technique was natural-reflex balancing with some manual assist for pitch controls. A light handhold on the rails or controls tended to smooth the operation and appeared to act as a damper in minimizing or preventing small oscillations. Most operators saw that a natural-balance routine was inadequate at the inertias of 600 and 900 slug-ft^2 (813 and 1220 kg-m^2) and used a manual-assist technique for all control. The conclusion by the authors is that inertia has two effects: one is a gradual degradation in handling qualities as inertia is increased; the other is a degradation as the operator is forced to change from a natural-type balance and control to a manual-assist technique between 300 and 600 slug-ft^2 (407 and 813 kg-m^2).

Varied platform elevation.- The foot platform was raised 1/2 foot (0.15 meter) and 1 foot (0.30 meter) by means of rigid step stools. The purpose of this test is to determine the effect of pilot vertical location on the handling qualities of the simulator. The data obtained with two operators (runs 33 to 35, and 37 to 39) were taken in the same time period to eliminate any effects of a learning curve on ratings. It should be noted, as

pointed out in the appendix, that raising the pilot center-of-gravity height from the simulator center of gravity introduces a mild simulator instability.

Operator T gave a rating of 3 at zero level and 3.5 at the other elevations. He downgraded the rating one-half a point because he had to reach down to the controls. Operator H gave the vehicle-pilot combination a rating of 3 at all three elevations. He did not reduce the rating because he had to stoop a little to the controls. In talking the matter over, it was agreed that other than the problem of reaching for the controls, there was no perceptible change in controllability because of a 1-foot (0.305-meter) vertical change in operator center-of-gravity location. The practice of changing operators without adjusting the platform to put his center of gravity exactly at the simulator center of gravity is therefore justified.

Backpack.- A 50-pound (222-newton) backpack illustrated in figure 11 was carried by operators T and H on the 600 slug-ft^2 (813 kg-m^2) configuration in runs 36 and 40 and may be compared with runs 33 and 37 made in the same time period without backpack. These runs were the only tests giving conflicting results between different operators. Operator T rated 3.5 with the backpack and 3 without because the backpack struck the vertical bars and interfered with his control. Operator J abandoned his test without a rating for the same reason. On the other hand, operator H rated a 2.5 to 3 with the backpack and a 3 without backpack. Realizing the interference problem he did not lean much but made effective use of the extra weight by pressing heavily with the toes or moving one foot as needed to any desired sector to obtain what he judged to be a quicker and more accurate response than without the added weight. This is the effect that was being looked for. However, all results are quite inconclusive because of mechanical difficulties and the different results obtained by different operators.

In any case, it is clear that a less restraining vehicle frame is required for compatibility with a backpack.

Auxiliary Platform

Dashpot optimization.- Early developmental trials with a spring-restrained undamped auxiliary platform resulted in an unacceptable platform jitter of several oscillations per second which was eliminated by the addition of two dashpots installed 90° apart. The original dashpots were found to be too stiff to give full pitch control in a second or less time. The smaller dashpot disks used in runs 3 to 8 allowed full pitch control, but the platform felt underdamped. In runs 9 to 50, a dashpot with a damping coefficient of $\frac{1.90 \text{ ft-lb}}{\text{deg/sec}} \left(\frac{2.58 \text{ m-N}}{\text{deg/sec}}\right)$ was used and operator consensus was that this amount of damping was satisfactory from I = 300 to 900 slug-ft^2 (407 to 1220 kg-m^2). However,

this damping was too low at 100 slug-ft^2 (136 kg-m^2) and the damping constant was adjusted to $\frac{4.60 \text{ ft-lb}}{\text{deg/sec}}\left(\frac{6.24 \text{ m-N}}{\text{deg/sec}}\right)$ for run 52, and on.

Effects of moment of inertia.- The test runs made with the auxiliary platform generally followed the natural-reflex balancing technique described in the section "Task and Techniques." Exceptions were some runs of operator T. The results are given in figure 12 for operators H, T, J, R, and W for the four values of inertia. Operator T purposely allowed the main frame to follow the auxiliary platform and made little effort to keep it upright. With this technique his ratings in runs 7, 4, and 13 at I = 300, 600, and 900 slug-ft^2 (407, 813, and 1220 kg-m^2) were on the high side of average, particularly in run 13 for which the point at I = 900 slug-ft^2 (1220 kg-m^2) is labeled "Learning point." Because of large oscillations of the main frame, it was rated 5. He repeated the test in run 13R by using the technique of maintaining the frame upright and made an exceptionally smooth run which he rated 3. This point is labeled "Proper technique." At I = 300 slug-ft^2 (407 kg-m^2), both runs rated 3.5 were with the underdamped platform. Both the 3 ratings at this inertia were with the more optimized damping, $\frac{1.90 \text{ ft-lb}}{\text{deg/sec}}\left(\frac{2.58 \text{ m-N}}{\text{deg/sec}}\right)$.

Except for the data points marked low damping and learning point, the dashed lines bound all the auxiliary platform data taken with symmetrical inertias. The solid line gives the mean of this data. Two things can be noticed. One is that the mean rating is satisfactory at all inertias. The other is that the mean data line shows only a small change in rating over the inertia range; only three-quarters of a rating point drop between an I of 100 slug-ft^2 and 900 slug-ft^2 (136 kg-m^2 and 1220 kg-m^2). Ratings of professional pilot W show no change in rating over this inertia range. This operator rated both the locked and unlocked platforms equal at a rating of 2 to 2.5 at I = 300 slug-ft^2 (407 kg-m^2) and remarked that he had no more trouble with these simulation runs, if as much, as with an ordinary helicopter flight.

Comparison of Locked and Unlocked Platforms

Figure 13 shows the mean data lines for the auxiliary platform and for the basic configuration. Although the auxiliary platform shows a superiority over the entire inertia range, this difference is only pronounced at the higher inertias of 600 and 900 slug-ft^2 (813 and 1220 kg-m^2). This difference is probably due to a greater degree of decoupling of the auxiliary platform from the main frame at the higher inertias where the handling quality assumes the desirable characteristic of becoming insensitive to inertia.

The superior controllability of the auxiliary platform configuration compared with the basic configuration was largely due to the easier prejudging and execution of maneuvers made possible by the almost instantaneous response of the auxiliary platform to a

control input. This rapid response is predictable on the basis of the low moment of inertia of the auxiliary platform.

The superiority of the auxiliary platform ratings appears to warrant the strong consideration of this type of control for a platform anywhere in the inertia range. As well as improving the pitch and roll control at design conditions, the auxiliary platform would make the design safe against emergency overload and permit a greater inertia growth factor for increasing vehicle operating range and weight.

Asymmetrical Configuration

Runs 59 to 63 were made with a moment of inertia of 300 slug-ft^2 (407 kg-m^2) in pitch and 1200 slug-ft^2 (1627 kg-m^2) in roll in the basic configuration or with the platform locked. The resultant pilot ratings of 2 to 3 are typical of a symmetrical configuration having I = 300 slug-ft^2 (407 kg-m^2) and suggest that the moment of inertia in roll is much less critical than the moment of inertia in pitch. Runs 64 to 66 made with the platform unlocked gave ratings of 2 to 2.5, values comparable with the unlocked platform in low-inertia symmetric distributions. The ratings indicate that the controllability of this configuration is very satisfactory. These results indicate that a logical flying-platform design for body-motion control is one with an auxiliary platform and propellant tanks located at either side.

Oscillations

Some measured values of the period of oscillation of the simulator are plotted in figure 14 along with a curve of period of oscillation computed by using equation (A36) and shown in figure 14. The test points, which were for amplitudes in the range of 3° to 5°, appear to verify the theory to within about 1/2 second. The simulator operator and flight vehicle pilot learn to avoid an oscillatory mode.

Pilot Ratings

The pilot ratings given in this program showed a wider range of values than is usually encountered in such a program, that is, a range of approximately 1.5 points as compared with the usual range of 0.5 point. This variation resulted from the differences in balance capability and experience of the test operators. This difference suggests that pilots of such a vehicle, particularly on early missions, should be chosen in part on the basis of a well-developed balance reflex.

CONCLUSIONS

One concept for a lunar flying platform is one in which the attitude control is obtained by a standing pilot who controls the vehicle by shifting his weight relative to the

thrust vector. A test program simulating the control of such a vehicle was conducted by shirt-sleeve operators using a variable-inertia simulator with five degrees of freedom, longitudinal and lateral translations, pitch, roll, and yaw, and one degree (altitude) simulated by instrument. Pitch and roll were obtained by mounting and mass balancing the simulator platform on a spherical segment; translations and yaw, by air bearings on a smooth flat floor; and the altitude simulation, by a control commanding rate of climb that was connected through a computer to an altimeter. Five-sixths of the weight was supported by air bearings on the floor and one-sixth of the weight was lifted by air jets which tilted with the vehicle to drive it about the floor with lunar accelerations and velocities. In an alternate control version, the jets were attached to a low-inertia auxiliary platform which could be tilted with respect to the rest of the vehicle. The primary purpose of the test program was to determine the effect of a wide range of moments of inertia on vehicle handling qualities and to test a simple countermeasure to high inertia, the auxiliary platform.

In the test program the vehicle moments of inertia were 100, 300, 600, and 900 slug-ft^2 (136, 407, 813, and 1220 kg-m^2) in pitch and roll and also 300 slug-ft^2 (407 kg-m^2) in pitch with 1200 slug-ft^2 (1627 kg-m^2) in roll. These values corresponded roughly to 33, 100, 200, 300 slug-ft^2 (45, 136, 271, 407 kg-m^2) and the combination 100 slug-ft^2 (136 kg-m^2) in pitch with 400 slug-ft^2 (542 kg-m^2) in roll for the lunar vehicle. Pilot ratings were assigned for a task involving a simulator translation of 26 feet (7.9 meters) from point to point. The indicated altitude was varied during the test. Although the ratings are not intended as absolute values, the trends are clear and significant. The test program and analysis developed the following conclusions:

1. This study has indicated that the natural-reflex control concept has a valid application to the design of lunar vehicles within the range of sizes investigated. Such vehicles should include an auxiliary control platform and have the fuel tanks located on the sides.

2. For the simulator without an auxiliary platform, the natural-reflex balancing technique for vehicle control was found to be satisfactory at inertias of 100 and 300 slug-ft^2 (136 and 407 kg-m^2) but inadequate at inertias of 600 and 900 slug-ft^2 (813 and 1220 kg-m^2). A learned manual-assist technique, usually done while holding on to handrails, was the preferred control method at these higher inertias.

3. Simulated flights with the auxiliary platform were satisfactory at all the inertias of the test, and definitely superior to the simulations with the platform locked at symmetrical moments of inertia of 600 and 900 slug-ft^2 (813 and 1220 kg-m^2). Natural-reflex body-motion control with a light handhold on the rails was preferred for this configuration. The easier prejudging and execution of maneuvers with the auxiliary platform were predictable on the basis of its low inertia and almost instantaneous angular response to a control input.

4. Tests with and without an auxiliary platform of a configuration having a moment of inertia of 300 slug-ft^2 (407 kg-m^2) in pitch and 1200 slug-ft^2 (1627 kg-m^2) in roll, an asymmetric inertia distribution thought to be representative of probable vehicle designs, resulted in pilot ratings comparable with those for the symmetrical configuration of 300 slug-ft^2 (407 kg-m^2) because body-motion control is more powerful in roll than in pitch. Again, the auxiliary platform configuration received the better pilot ratings.

5. Tests for the effect of carrying a 50-pound (222-newton) backpack were limited and generally inconclusive because of interference between the pack and vertical rails. However, one test operator who did not encounter this interference noticed improved control performance.

6. A 1-foot (0.305-meter) change of pilot vertical location relative to the center of gravity of the simulator caused no change in pilot rating or task difficulty beyond the inconvenience of reaching down to the hand controls; thus, variations in the stature of the test operators did not appreciably affect the results.

Langley Research Center,
National Aeronautics and Space Administration,
Hampton, Va., August 24, 1970.

APPENDIX

MATHEMATICAL ANALYSIS OF LUNAR TRANSPORT VEHICLE AND SIMULATOR

The quality of any simulation depends on the simulator's response to operator input. In other words, for a good simulation, the response of the simulator to any given operator input should duplicate the response of the vehicle being simulated.

The following analysis, comparing the simulator forces, moments, and motions with those of a jet-supported flying platform, is presented to show that the angular acceleration of the simulator due to operator input and the linear acceleration due to simulator tilt angle are accurate representations of a jet-supported flying platform in a reduced-gravity field.

Basic Configuration

A comparative analysis of the basic lunar transport vehicle and simulator configurations is presented.

Control moments.- A comparison of the control moments generated by the operator on a jet-supported flying platform and the basic simulator is presented in figure 15. The flying-platform control moment Q_v results from displacement of the center of mass of the operator from its neutral position along the thrust axis (see fig. 15(a)) and may be written as

$$Q_v = F_{i,m} e_m \tag{A1}$$

where the inertia force of the operator parallel to the thrust axis $F_{i,m}$ is equal to the mass of the operator times the acceleration of the vehicle-operator combination along the thrust axis and may be written as the ratio of the operator weight W_m to total vehicle weight $W_v + W_m$ times the vehicle thrust as

$$F_{i,m} = \frac{W_m}{W_v + W_m} T_v \tag{A2}$$

Substituting equation (A2) into equation (A1) gives

$$Q_v = \frac{T_v}{W_{t,v}} W_m e_m \tag{A3}$$

It might be noted from this equation that control moment is a function of thrust level, as would be expected.

APPENDIX

For the simulator the control moment results from the displacement of the operator's weight with respect to the radius from the center of curvature of the spherical surface to the point of contact between the spherical surface and the flat plate (see fig. 15(b)) and may be written as

$$Q_S = W_m e_m \cos \theta_S + F_{i,m} e_m \sin \theta_S - W_b l \sin \theta_S + F_{i,b} l \cos \theta_S + F_{i,d} R \qquad \text{(A4a)}$$

where to obtain control moments only from the input of the operator, the summation of ballast and air-pad-dolly terms must equal zero. Equation (A4a) then reads

$$Q_S = W_m e_m \cos \theta_S + F_{i,m} e_m \sin \theta_S \qquad \text{(A4b)}$$

The presence of the sine and cosine functions of the tilt angle θ_S changes the control capability of the operator for a given body displacement from the neutral position by less than 2 percent for the range of 0^o to 13^o tilt angles available on the simulator and by 1 percent at 10^o for a 165-pound (734-newton) operator.

It should be noted that with a pressure suit and backpack, the earth weight of an operator of the flying platform would be approximately twice his shirt-sleeve weight; therefore, the ratio of lunar to earth weight of the operator is approximately 1 to 3. This ratio is further modified by the thrust level of the flying platform, as noted above, when control inputs by the operator are computed.

If the center of gravity of the simulator operator is placed above the center of curvature by an amount d_o, measured along the simulator thrust axis, two additional terms would be introduced in equations (A4a) and (A4b). These terms are:

$$W_m d_o \sin \theta_S - F_{i,m} d_o \cos \theta_S$$

The elimination of $F_{i,m}$ by the simulator equivalent of equation (A2) reduces these additional terms to the expression:

$$W_m d_o \sin \theta_S \left(1 - \frac{T_S}{W_{t,s}} \cos \theta_S\right)$$

An inspection of equation (A1) shows that these terms should not be present, or that the operator's center of gravity should be at the center of curvature. Placing the center of gravity of the operator above the center of curvature introduces an instability. This instability can be visualized physically, since placing the center of gravity above the center of curvature of a sphere must make it topheavy. However, experimental evaluation of the effect of gross operator displacements, on the order of 1 foot (0.30 meter), on simulator controllability have shown negligible if any degradation from this source.

Therefore, this component of simulator control moment has not been included in this analysis.

Translational acceleration.- The horizontal accelerations of the flying platform and the basic simulator, resulting from their components of thrust in the horizontal plane, may be obtained from figures 15(a) and 15(b), respectively. For the flying platform,

$$a_V = \frac{T_V \sin \theta_V}{W_{t,v}/g_e} \tag{A5}$$

and for the simulator,

$$a_S = \frac{T_S \sin \theta_S}{W_{t,s}/g_e} \tag{A6}$$

To reproduce the flying-platform motions for a given tilt-angle time history, the simulator acceleration must equal the flying-platform acceleration; therefore, combining equations (A5) and (A6) gives the expression for the thrust-weight ratios:

$$\frac{T_S}{W_{t,s}} = \frac{T_V}{W_{t,v}} \tag{A7}$$

Rotational acceleration.- The angular (tilt angle) acceleration of the flying platform resulting from an operator control torque may be written as follows (see fig. 15):

$$\ddot{\theta}_V = \frac{Q_V}{I_V + \frac{W_V}{g_e} d_V^2 + I_m + \frac{W_m}{g_e} d_m^2} \tag{A8}$$

where d_V and d_m are the respective distances of the center of gravity of the vehicle and operator from their common center of gravity. The ratio of d_V to d_m is the inverse of the ratio of vehicle mass to operator mass. The control torque Q_V is given by equation (A3).

The equation for the angular acceleration of the simulator about the center of curvature is as follows:

$$\ddot{\theta}_S = \frac{Q_S}{I_S + \frac{W_b}{g_e} l^2 + \frac{W_d}{g_e} R^2 + I_m + \frac{W_m}{g_e} e_m^2} \tag{A9}$$

The denominator may be considered to be an effective moment of inertia in which the ballast weight term $\frac{W_b}{g_e} l^2$ results from the addition of a ballast weight to the simulator to achieve a value of positive static stability necessary to attain a neutral dynamic stability as the simulator accelerates in translation. Without the ballast weight, the simulator is dynamically unstable because of the inertia of the dolly. The inertia of the dolly appears in the effective inertia of the simulator as the term $\frac{W_d}{g_e} R^2$. Setting the ballast and dolly terms equal to zero in equation (A4a) yields:

$$-W_b l \sin \theta_s + F_{i,b} l \cos \theta_s + F_{i,d} R = 0 \tag{A10}$$

where

$$F_{i,b} = \frac{W_b}{g_e} a_s \tag{A11}$$

$$F_{i,d} = \frac{W_d}{g_e} a_s \tag{A12}$$

The inertia forces $F_{i,b}$ and $F_{i,d}$ may be written as ratios of ballast and dolly weights W_b and W_d, respectively, to total simulator weight $W_{t,s}$ times the simulator horizontal thrust component:

$$F_{i,b} = \frac{W_b}{W_{t,s}} T_s \sin \theta_s \tag{A13}$$

$$F_{i,d} = \frac{W_d}{W_{t,s}} T_s \sin \theta_s \tag{A14}$$

Substituting equations (A13) and (A14) into equation (A10) gives

$$W_b l \sin \theta_s - \frac{W_b}{W_{t,s}} T_s l \sin \theta_s \cos \theta_s - \frac{W_d}{W_{t,s}} T_s R \sin \theta_s = 0$$

and reducing this equation yields

$$W_b l = \frac{T_s / W_{t,s}}{1 - \frac{T_s}{W_{t,s}} \cos \theta_s} W_d R \tag{A15}$$

The ballast-weight effect due to tilt angle may be neglected because over the usable range of tilt angles the variation was less than 3 percent. Also, since, for this test

program, only moderate deviations from the lunar hovering case $\left(\text{that is, } \frac{T_s}{W_{t,s}} = \frac{1}{6}\right)$ were used, a single value and position of ballast weight were used.

Auxiliary Platform Configuration

The following analysis compares the rotational and linear acceleration equations of motion for a flying platform and simulator having an auxiliary platform mounted as previously described to provide more effective control response for high-inertia vehicles. (See fig. 16.)

Control moments.- From figure 16(a) the control moment produced by the operator on the lunar-vehicle auxiliary platform when moments are taken about the platform pivot point is as follows:

$$Q_{a,v} = F_{i,m}e_m - K_{s,v}\gamma_v - K_{d,v}\dot{\gamma}_v \tag{A16}$$

where $K_{s,v}$ and $K_{d,v}$ are the spring and damping constants, respectively, between the auxiliary platform and the main, high-inertia frame of the lunar vehicle and γ_v is the angular displacement of the auxiliary platform with respect to the center line of the main frame.

From figure 16(b) the comparable control moment for the simulator about the pivot point is

$$Q_{a,s} = W_m\left[\left(l_p + l_m \cos\delta\right)\sin\theta_s + l_m \sin\delta\cos\theta_s\right] - F_{i,m}\left[\left(l_p + l_m\cos\delta\right)\cos\theta_s - l_m\sin\delta\sin\theta_s\right] + W_a l_a \sin\theta_s - F_{i,a}l_a\cos\theta_s - K_{s,s}\gamma_s - K_{d,s}\dot{\gamma}_s \tag{A17}$$

Taking moments acting about the respective center of gravities of the main frame gives

$$Q_{f,v} = -T_v l_f \sin\gamma_v + F_{i,m}l_f\sin\gamma_v + F_{i,a}l_f\sin\gamma_v + K_{s,v}\gamma_v + K_{d,v}\dot{\gamma}_v \tag{A18}$$

for the lunar vehicle and

$$Q_{f,s} = -T_s l_f \sin\gamma_s - W_m l_f \sin\beta_s - W_a l_f \sin\beta_s + F_{i,m}l_f\cos\beta_s + F_{i,a}l_f\cos\beta_s - W_b\left(l_b + l_f\right)\sin\beta_s + F_{i,b}\left(l_b + l_f\right)\cos\beta_s + F_{i,d}R + K_{s,s}\gamma_s + K_{d,s}\dot{\gamma}_s \tag{A19a}$$

for the simulator. Here, as for the basic configuration, the summation of ballast and air-pad-dolly terms must equal zero. Equation (A19a) then reads

$$Q_{f,s} = -T_s l_f \sin \gamma_s - W_m l_f \sin \beta_s - W_a l_f \sin \beta_s + F_{i,m} l_f \cos \beta_s + F_{i,a} l_f \cos \beta_s$$

$$+ K_{s,s}\gamma_s + K_{d,s}\dot{\gamma}_s \tag{A19b}$$

Translational accelerations.- The translational accelerations of the lunar vehicle and simulator may be expressed similar to the basic configurations; thusly,

$$a_v = \frac{T_v \sin \theta_v}{W_{t,v}/g_e} \qquad \left(W_{t,v} = W_v + W_m\right)$$

$$a_s = \frac{T_s \sin \theta_s}{W_{t,s}/g_e}$$

Rotation of thrust line.- The rotation of the line of thrust of the lunar vehicle and simulator are obtained from similar equations (see fig. 16):

$$\theta_v = \beta_v + \gamma_v \tag{A20}$$

$$\theta_s = \beta_s + \gamma_s \tag{A21}$$

where

$$\ddot{\gamma}_v = \frac{Q_{a,v}}{I_a + \frac{W_a}{g_e} l_a^2 + I_m + \frac{W_m}{g_e}\left(l_p^2 + 2 l_p l_m \cos \delta + l_m^2\right)} \tag{A22}$$

and

$$\ddot{\gamma}_s = \frac{Q_{a,s}}{I_a + \frac{W_a}{g_e} l_a^2 + I_m + \frac{W_m}{g_e}\left(l_p^2 + 2 l_p l_m \cos \delta + l_m^2\right)} \tag{A23}$$

Likewise the tilt angle of the main frames may be written as

$$\ddot{\beta}_v = \frac{Q_{f,v}}{I_{f,v} + \frac{W_m}{g_e} l_f^2 + \frac{W_a}{g_e} l_f^2} \tag{A24}$$

and

$$\ddot{\beta}_s = \frac{Q_{f,s}}{I_{f,s} + \frac{W_m}{g_e} l_f^2 + \frac{W_a}{g_e} l_f^2 + \frac{W_b}{g_e}\left(l_b + l_f\right)^2 + \frac{W_d}{g_e} R^2} \tag{A25}$$

APPENDIX

If the foregoing equations are satisfied and if the control input of the simulator operator matches the time history of the control inputs of the flight-vehicle operator, the time histories of the simulator auxiliary platform and main frame angles γ_S and β_S will match the corresponding time histories of the flight-vehicle angles γ_V and β_V. For practical purposes the control-angle inputs are essentially instantaneous and thus two integrations are eliminated. If T/M is assumed to be constant, and θ is the pitch attitude of the auxiliary platform as well as of the jets, performancewise the equations of motion during constant acceleration are

$$\left.\begin{aligned} M\ddot{x} &= T_V \sin\theta \\ M\dot{x} &= T_V t \sin\theta \\ Mx &= \frac{T_V t^2}{2} \sin\theta \end{aligned}\right\} \tag{A26}$$

Oscillations

Magnitude.- It is, of course, desirable to put in a control-moment sequence in pitch or roll which would "deadbeat" the vehicle to a desired new attitude. This condition can be accomplished by putting in a positive control moment to give the vehicle some angular velocity in pitch or roll and then an equal negative input to stop the vehicle at the desired attitude. If the vehicle is overcontrolled and overshoots the desired attitude and a second negative input is made to bring the attitude back, a rocking motion may ensue. It is instructive to an understanding of this type of vehicle to look at the equations of such an oscillating motion. The equations have a simple solution for a steady sinusoidal rocking induced by a sinusoidal moment input by the operator. Let the moment input have a maximum value of Q_{max} and an impressed frequency of ω. Equating the product of moment of inertia I and angular acceleration $\ddot{\theta}$ to the instantaneous value of the moment gives

$$Q = I\ddot{\theta} = Q_{max} \sin\omega t \tag{A27}$$

Integrating with respect to time for the initial conditions shown in sketch (b)

$$\dot{\theta} = -\frac{Q_{max}}{I\omega} \cos\omega t \tag{A28}$$

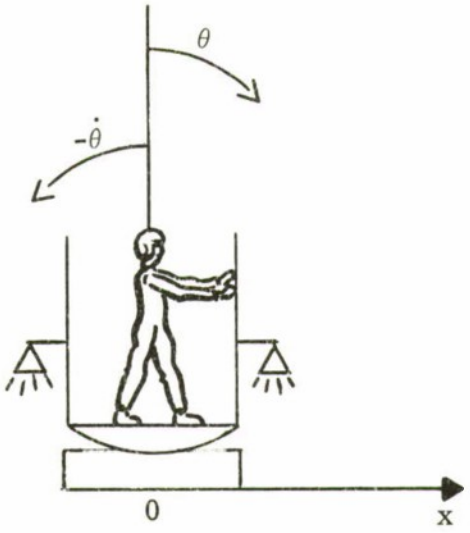

$$\dot{\theta} = -\frac{Q_{max}}{I\omega} \quad \text{at} \quad t = 0$$

$$\dot{x} = \frac{T}{M}\frac{Q_{max}}{I\omega^3} \quad \text{at} \quad t = 0$$

$\theta = 0$ in position shown at $t = 0$

$Q = 0$ in position shown at $t = 0$

Sketch (b)

As seen by equation (A28) at time zero, the vehicle is rocking counterclockwise with the angular velocity equal to $-Q_{max}/I\omega$ and at this time the operator begins his positive moment $Q_{max} \sin \omega t$ as shown by equation (A27). Integrating equation (A28)

$$\theta = -\frac{Q_{max}}{I\omega^2} \sin \omega t \tag{A29}$$

The lifting jets are alined perpendicular to the vehicle platform. The horizontal component of force for small angles is approximately equal to the product of thrust T and angle θ from equation (A29). Equating mass times acceleration to the horizontal force yields

$$M\ddot{x} = -T\frac{Q_{max}}{I\omega^2} \sin \omega t \tag{A30}$$

Integrating, T/M being assumed constant, yields

$$\dot{x} = \frac{T}{M}\frac{Q_{max}}{I\omega^3} \cos \omega t \tag{A31}$$

and integrating again yields

$$x = \frac{T}{M}\frac{Q_{max}}{I\omega^4} \sin \omega t \tag{A32}$$

APPENDIX

In the current series of experiments T/M is set at or near 1/6 earth g or about 5.4 ft/sec^2 (1.65 m/sec^2). For a given θ_{max}, equation (A29), and a given frequency ω, it can be seen from equation (A32) that horizontal excursions on the moon and on any proper simulation will be one-sixth as great as those for an earth flying platform or an earth simulator where thrust equals weight and T/M = 32.2 ft/sec^2 (9.81 m/sec^2).

Figure 17 shows plots for Q, $\dot{\theta}$, θ, $\dot{x}$, and x calculated from the preceding equations for T/M = 5.4 ft/sec^2 (1.65 m/sec^2), a moment of inertia I = 600 slug-ft^2 (813 kg-m^2), a maximum control input Q_{max} = 100 lb-ft (136 N-m), and a frequency ω = 0.897 rad/sec corresponding to a period of 7 seconds. This frequency is typical for the pilot-simulator combination at this inertia. Inspection of the equations shows that the magnitudes of the angular and horizontal excursions are proportional to the magnitude of the forced inputs.

The main thing to notice in the equations of motion is that from the time a control moment is initiated by the operator, four integrations with respect to time are required before the resulting displacements in distance are obtained. Sinusoidal partial-wave inputs are not a good basis for practical operation as four mental integrations of such an input would be difficult for the pilot to predict.

Period.- As indicated in the preceding section, an oscillating platform can be forced at any frequency ω imposed by the body motions of the operator. However, if the operator of an oscillating vehicle fixes his body axis in inertial space the vehicle will have a resonant frequency dependent on the physical properties of the vehicle, operator, and acceleration field. This result has been noticed in previous flight and simulator experiments and in the present test program.

From figure 1, the moment input for the simulator or a lunar flyer is

$$Q = W_e l_m \sin \theta \tag{A33}$$

It is assumed that the operator holds his body fixed in space and the vehicle is rocking so that

$$Q_{max} = W_e l_m \sin \theta_{max} \tag{A33a}$$

Equation (A29) was

$$\theta = -\frac{Q_{max}}{I\omega^2} \sin \omega t$$

Substitute equation (A33a) into equation (A29) and let $\omega t = \frac{3}{2}\pi$ and $\sin \omega t = -1$ for a maximum value of θ

$$\theta_{max} = \frac{W_e l_m \sin \theta_{max}}{I\omega^2}$$

from which the frequency is

$$\omega = \sqrt{\frac{W_e l_m \sin \theta_{max}}{I\theta_{max}}} \tag{A34}$$

and the period P is

$$P = \frac{2\pi}{\omega} = 2\pi\sqrt{\frac{I\theta_{max}}{W_e l_m \sin \theta_{max}}} \tag{A35}$$

For small amplitudes

$$P = 2\pi\sqrt{\frac{I}{W_e l_m}} \tag{A36}$$

which is the torsion-pendulum equation with $W_e l_m$ as the spring constant. The curve in figure 14 is a plot of equation (A36). The test points, which were for amplitudes in the range of 3^o to 5^o, appear to verify the theory within about 1/2 second.

REFERENCES

1. Thomas, David F.; and Hill, Paul R.: Lunar Flying Platform Simulator. NASA TN D-6001, 1970.

2. Hill, Paul R.; and Kennedy, T. L.: Flight Tests of a Man Standing on a Platform Supported by a Teetering Rotor. NACA RM L54B12a, 1954.

3. Zimmerman, C. H.; Hill, Paul R.; and Kennedy, T. L.: Preliminary Experimental Investigation of the Flight of a Person Supported by a Jet Thrust Device Attached to His Feet. NACA RM L52D10, 1953.

4. Cooper, George E.; and Harper, Robert P., Jr.: The Use of Pilot Rating in the Evaluation of Aircraft Handling Qualities. NASA TN D-5153, 1969.

TABLE I.- PILOT RATING SCALE

Adjective rating	Numerical rating	Description
Satisfactory	1	Excellent, includes optimum
	2	Good, pleasant to fly
	3	Satisfactory, but with some mildly unpleasant characteristics
Acceptable	4	Acceptable, but with unpleasant characteristics
	5	Unacceptable for normal operation
	6	Acceptable for emergency condition only
Unacceptable	7	Unacceptable, even for emergency condition
	8	Unacceptable – dangerous
	9	Unacceptable – uncontrollable
Unflyable	10	Unflyable

TABLE II.- INDEX RELATING CONFIGURATIONS AND RESULTS

Run	Moment of inertia in roll		Moment of inertia in pitch		Operating pressure		Auxiliary control	Position of operator's feet	Pilot	Pilot rating	Figure	Miss distance		Run time, second
	slug-ft^2	kg-m^2	slug-ft^2	kg-m^2	psi	kN/m^2						feet	meters	
1	600	813	800	813	300	2068.5	Locked	On platform	T	4.5	10	1, 1.5	0.30, 0.48	42
2	600	813	600	813	300	2068.5	Locked	On platform	J	4, 4.5	10	.5	.15	28
**3	600	813	600	813	370	2551.2	Operable	On platform	J	3	12	.5	.15	28
**4	600	813	600	813	370	2551.2	Operable	On platform	T	3.5	12	.5	.15	35
**5	600	813	600	813	370	2551.2	Operable	On platform	H	3	12	.5	.15	32
**8	300	407	300	407	370	2551.2	Operable	On platform	J	-----	--	.75	.23	28
**7	300	407	300	407	370	2551.2	Operable	On platform	T	3.5	12	1	.30	35
**8	300	407	300	407	370	2551.2	Operable	On platform	H	3.5	12	1	.30	33
9	300	407	300	407	370	2551.2	Operable	On platform	J	-----	--	5	.15	32
10	300	407	300	407	370	2551.2	Operable	On platform	T	3	12	.75	.23	--
11	300	407	300	407	370	2551.2	Operable	On platform	H	3	12	1	.30	33
12	900	1220	900	1220	370	2551.2	Operable	On platform	J	2.5	12	.5	.15	35
13	900	1220	900	1220	370	2551.2	Operable	On platform	T	5	12	2	.61	45
13R	900	1220	900	1220	370	2551.2	Operable	On platform	T	3	12	.5	.15	35
14	900	1220	900	1220	370	2551.2	Operable	On platform	H	3.5	12	.75	.23	39
15	900	1220	900	1220	370	2551.2	Operable	On platform	J	3	12	.25	.08	37
16	900	1220	900	1220	370	2551.2	Operable	On platform	T	3	12	.25	.08	38
17	900	1220	900	1220	370	2551.2	Operable	On platform	H	3	12	.25	.08	33
18	900	1220	900	1220	370	2551.2	Locked	On platform	J	3.5, 5	10	1	.30	--
19	900	1220	900	1220	370	2551.2	Locked	On platform	T	4	10	.75	.23	40
20	900	1220	900	1220	370	2551.2	Locked	On platform	H	5, 3.5	10	.5	.15	43
21	600	813	600	813	370	2551.2	Locked	On platform	T	4	10	1	.30	52
22	600	813	800	813	340	2344.3	Locked	On platform	J	3	10	0	0	43
23	600	813	600	813	340	2344.3	Locked	On platform	H	3.5	10	.25	.08	42
24	600	813	600	813	340	2344.3	Locked	On platform	J	3	10	.125	.04	38
25	600	813	600	813	340	2344.3	Locked	On platform	H	3.5	10	.25	.08	33
26	300	407	300	407	370	2551.2	Locked	On platform	W	2, 2.5	10	.25	.08	45
27	600	813	800	813	370	2551.2	Locked	On platform	W	3.5, 4	10	1	.30	46
28	900	1220	900	1220	370	2551.2	Locked	On platform	W	4	10	.75	.23	38
29	900	1220	900	1220	370	2551.2	Operable	On platform	W	2, 2.5	12	1.5	.46	33
30	600	613	600	813	370	2551.2	Operable	On platform	W	2, 2.5	12	2	.81	21 to 40
31	300	407	300	407	370	2551.2	Operable	On platform	W	2, 2.5	12	2	.61	18
32	300	407	300	407	370	2551.2	Operable	On platform	W	2	--	.125	.04	30
33	600	813	600	813	370	2551.2	Locked	On platform	T	3	10	.25	.08	48
34	600	813	600	813	370	2551.2	Locked	+1/2 ft (0.15 m)	T	3.5	--	.25	.08	45
35	600	813	600	813	370	2551.2	Locked	+1 ft (0.30 m)	T	3	--	.25	.08	47
*36	600	813	600	813	370	2551.2	Locked	On platform	T	3.5	--	.125	.04	45
37	600	813	600	813	370	2551.2	Locked	On platform	H	3	10	.5	.15	33
38	800	813	600	813	370	2551.2	Locked	+1/2 ft (0.15 m)	H	3	--	.25	.08	32
39	600	813	600	813	370	2551.2	Locked	+1 ft (0.30 m)	H	3	--	.25	.08	33
*40	600	813	600	813	370	2551.2	Locked	On platform	H	2.5, 3	--	.25	.08	30
41	300	407	300	407	370	2551.2	Locked	On platform	J	3	10	0.25, 0.5	0.08, 0.15	33
42	300	407	300	407	370	2551.2	Locked	On platform	H	3.5	10	0.25, 0.5	0.08, 0.15	38
43	100	138	100	136	350	2413.3	Locked	On platform	T	2, 2.5	10	.25	.08	27
44	100	136	100	136	350	2413.3	Locked	On platform	H	2	10	.375	.11	31
45	100	136	100	138	350	2413.3	Locked	On platform	J	2.5	10	.25	.08	30
**46	100	136	100	136	350	2413.3	Operable	On platform	T	1.5	12	0	0	22
**47	100	136	100	138	350	2413.3	Operable	On platform	H	2	12	.25	.08	20
**48	100	136	100	136	350	2413.3	Operable	On platform	J	2	12	.25	.08	19
49	100	138	100	136	350	2413.3	Locked	On platform	R	3	10	.75	.23	30
**50	100	138	100	136	350	2413.3	Operable	On platform	R	4	12	1	.30	20
***51	100	138	100	136	350	2413.3	Operable	On platform	R	4	12	1	.30	22
52	100	136	100	136	350	2413.3	Operable	On platform	R	2.5	12	0	0	19
53	100	138	100	136	350	2413.3	Operable	On platform	H	2.5	12	.25	.08	20
54	100	136	100	136	350	2413.3	Operable	On platform	J	2	12	.125	.04	22
55	100	136	100	138	350	2413.3	Locked	On platform	W	2	10	1	.30	20
56	100	136	100	138	350	2413.3	Operable	On platform	W	2, 2.5	12	1	.30	15
57	100	136	100	136	350	2413.3	Operable	On platform	H	2	12	.5	.15	18
58	100	136	100	136	350	2413.3	Operable	On platform	J	2	12	.5	.15	15
59	300	407	1200	1627	370	2551.2	Locked	On platform	T	2	--	.5	.15	43
60	300	407	1200	1627	370	2551.2	Locked	On platform	H	2.5, 3	--	.5	.15	40
81	300	407	1200	1627	370	2551.2	Locked	On platform	J	2.5, 3	--	.5	.15	29
62	300	407	1200	1827	370	2551.2	Locked	On platform	T	2, 2.5	--			30
63	300	407	1200	1627	370	2551.2	Locked	On platform	J	2.5	--	.5	.15	30
84	300	407	1200	1827	370	2551.2	Operable	On platform	H	2, 2.5	--	.25	.08	37
85	300	407	1200	1627	370	2551.2	Operable	On platform	T	2	--	.25	.08	35
66	300	407	1200	1627	370	2551.2	Operable	On platform	J	2	--	.25	.08	23

*With backpack.
**Underdamped.
***Overdamped.

TABLE III.- PILOT CHARACTERISTICS AND EXPERIENCE

Code symbol	Data symbol	Weight		Height		Helicopter pilot	Aircraft pilot	Spacecraft simulations	Research engineer
		lb	N	ft and in.	m				
H	○	165	734	6'0"	1.83	No	No	Yes	Yes
T	◇	175	778	5'10"	1.78	No	Light planes	Yes	Yes
J	□	165	734	5'9"	1.75	No	No	No	No
W	▷	170	756	6'0"	1.83	Test pilot	Test pilot	Yes	Yes
R	◺	160	712	5'10"	1.78	Test pilot	Test pilot	Yes	Yes

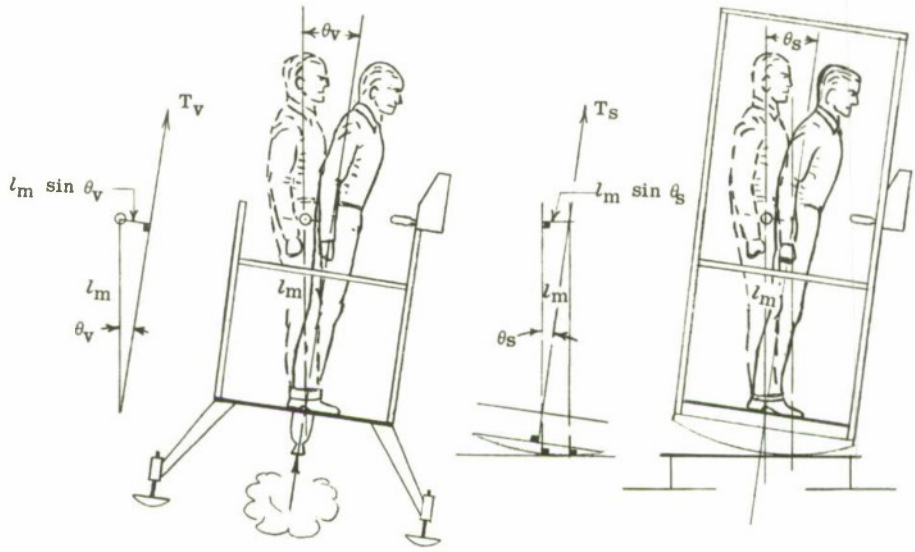

(a) Lunar flying platform. (b) Simulator.

Figure 1.- Balance principle as applied to jet-supported flying platform and simulator.

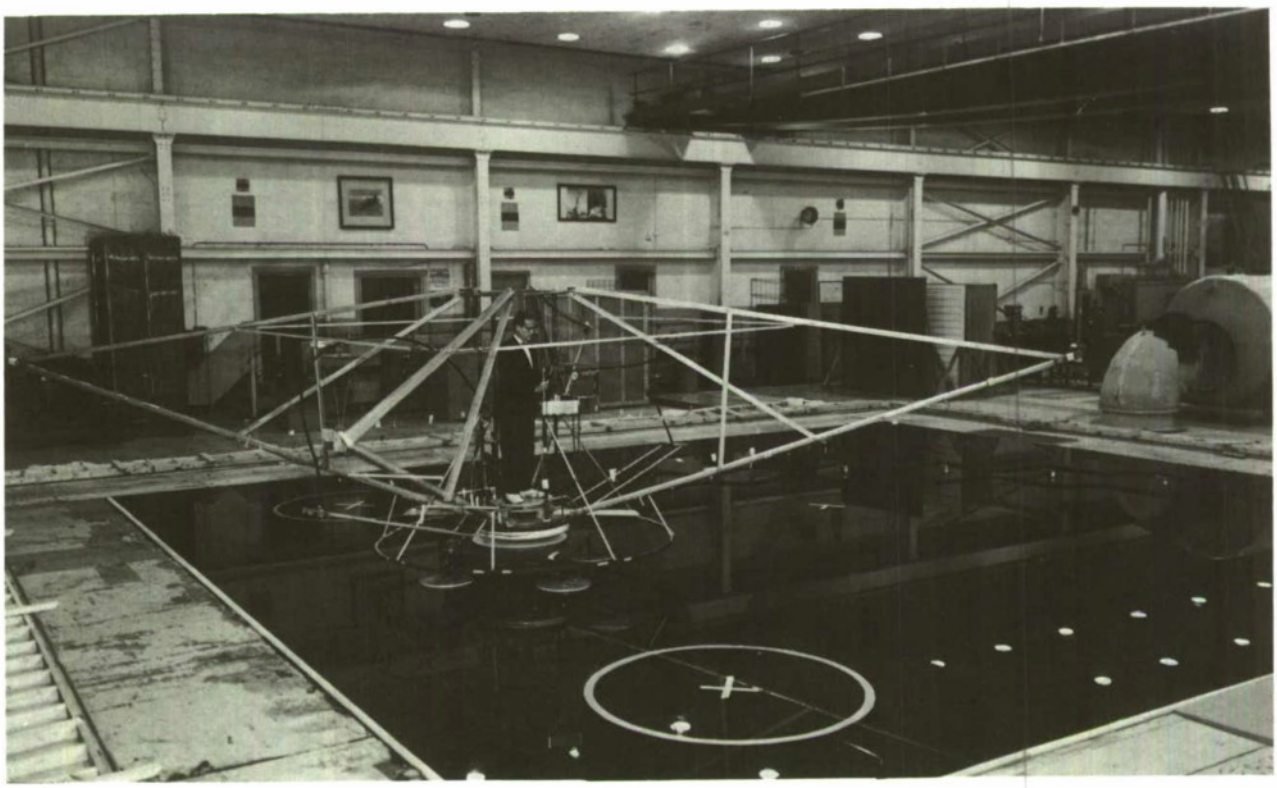

L-70-2718

Figure 2.- Overview of lunar-flying-platform simulator.

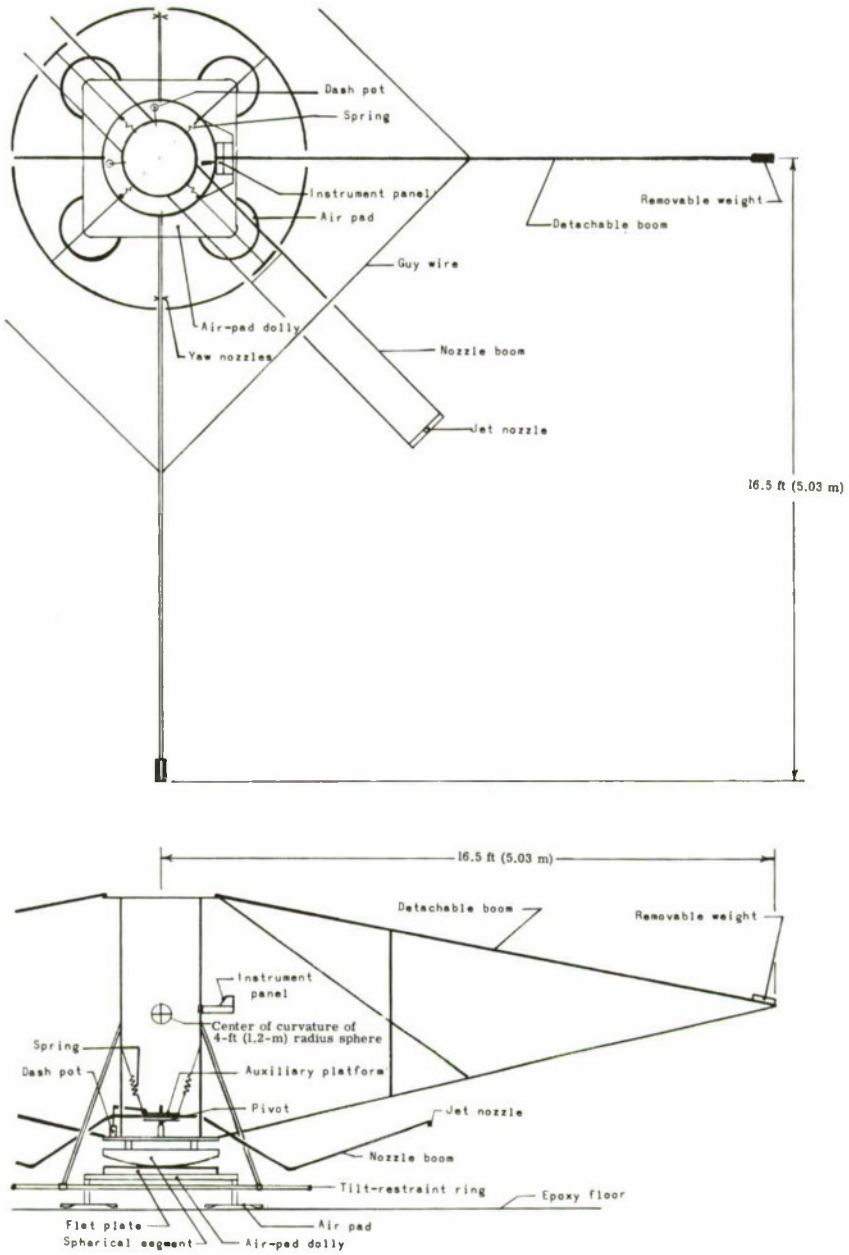

Figure 3.- Simplified sketch of simulator construction.

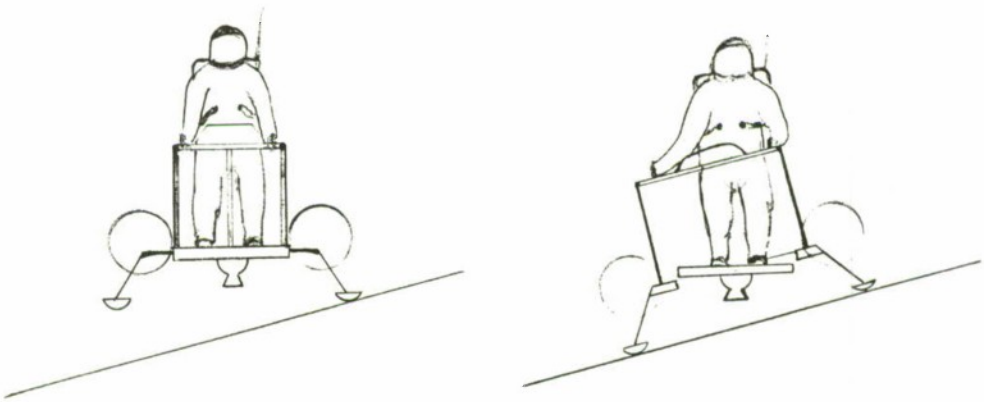

(a) Basic configuration. (b) Auxiliary platform configuration.

Figure 4.- Landing on a slope.

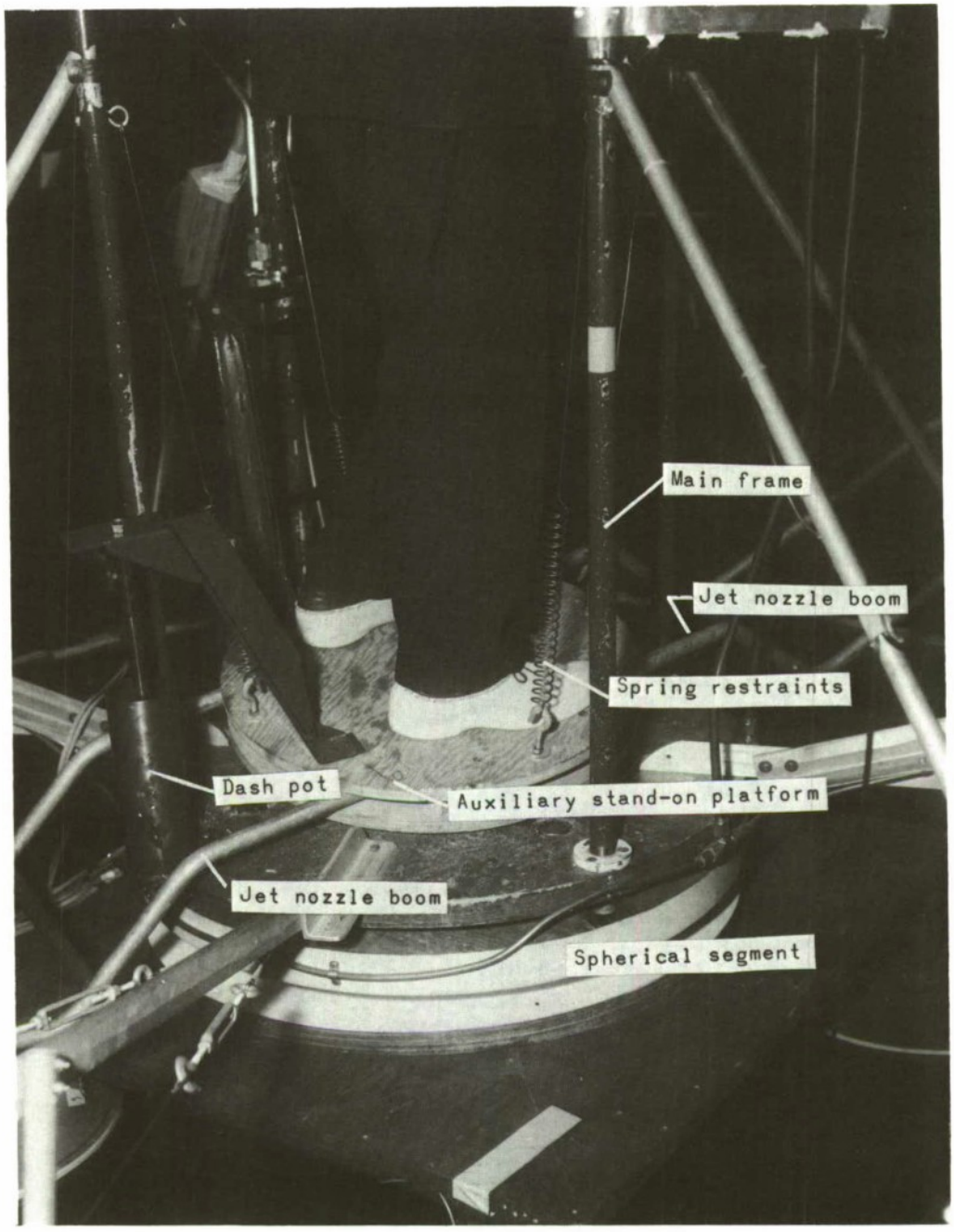

L-70-2724.1

Figure 5.- Auxiliary platform configuration with platform deflected.

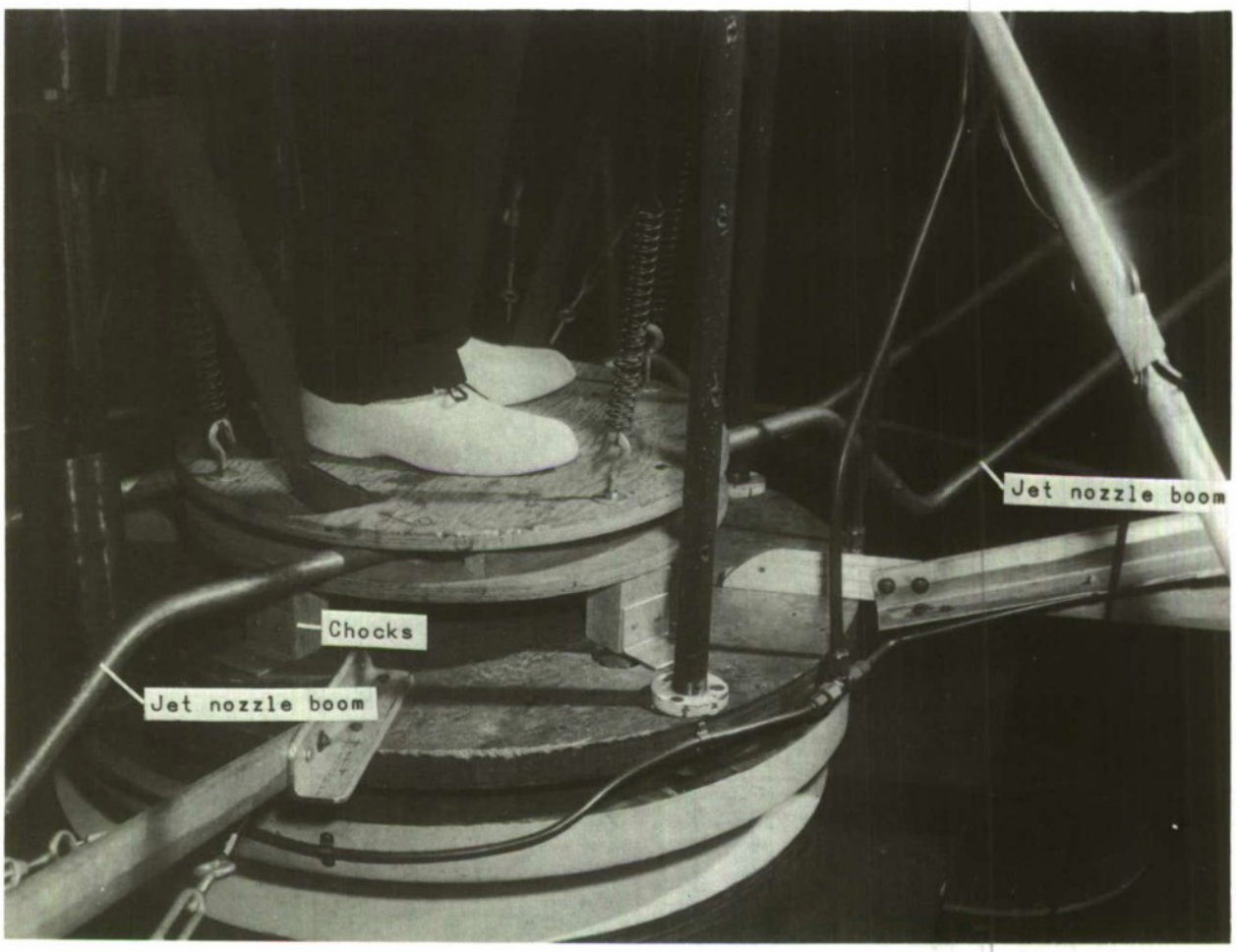

L-70-2721.1

Figure 6.- Closeup of basic configuration with auxiliary platform chocked.

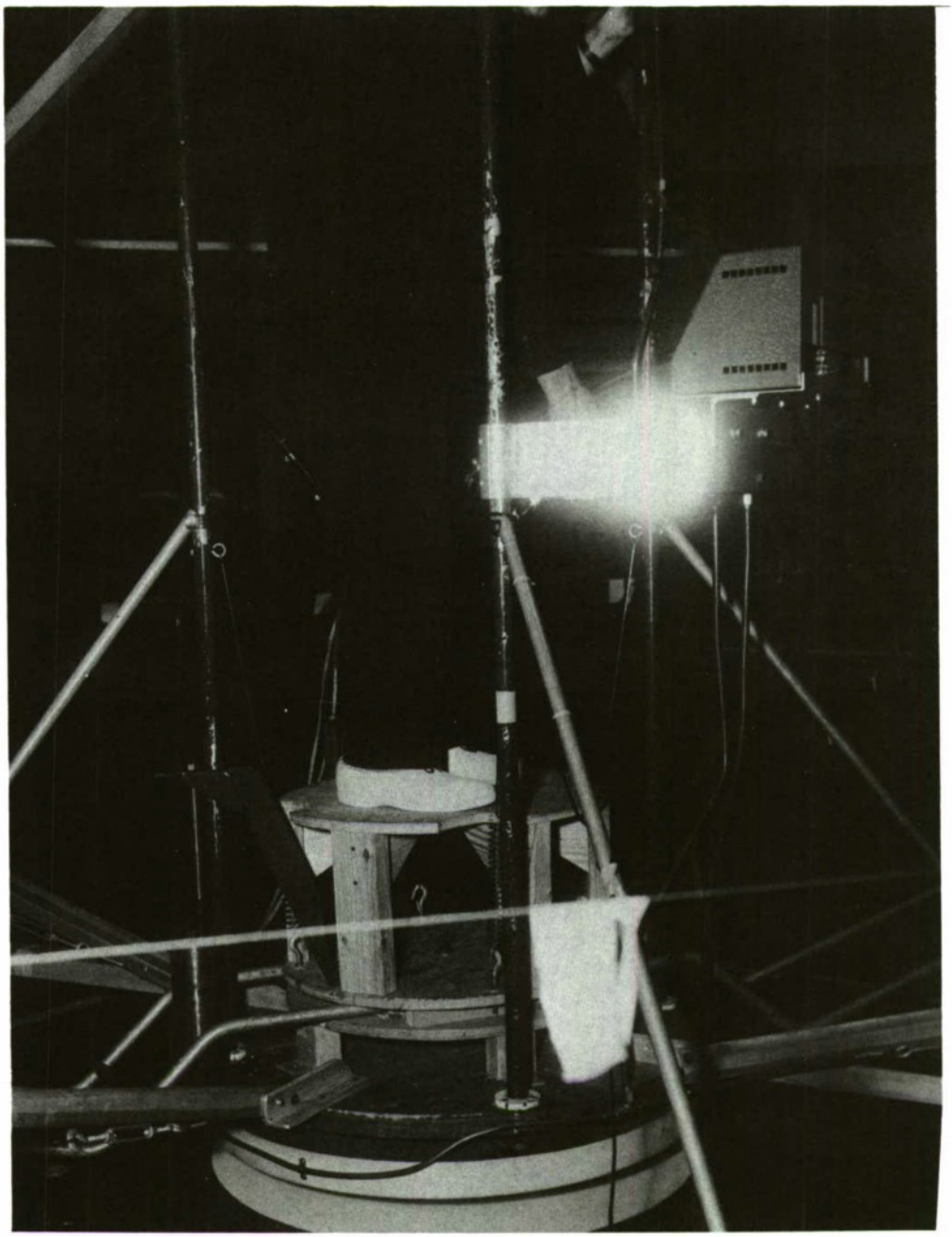

L-70-2723

Figure 7.- Variable platform height configuration.

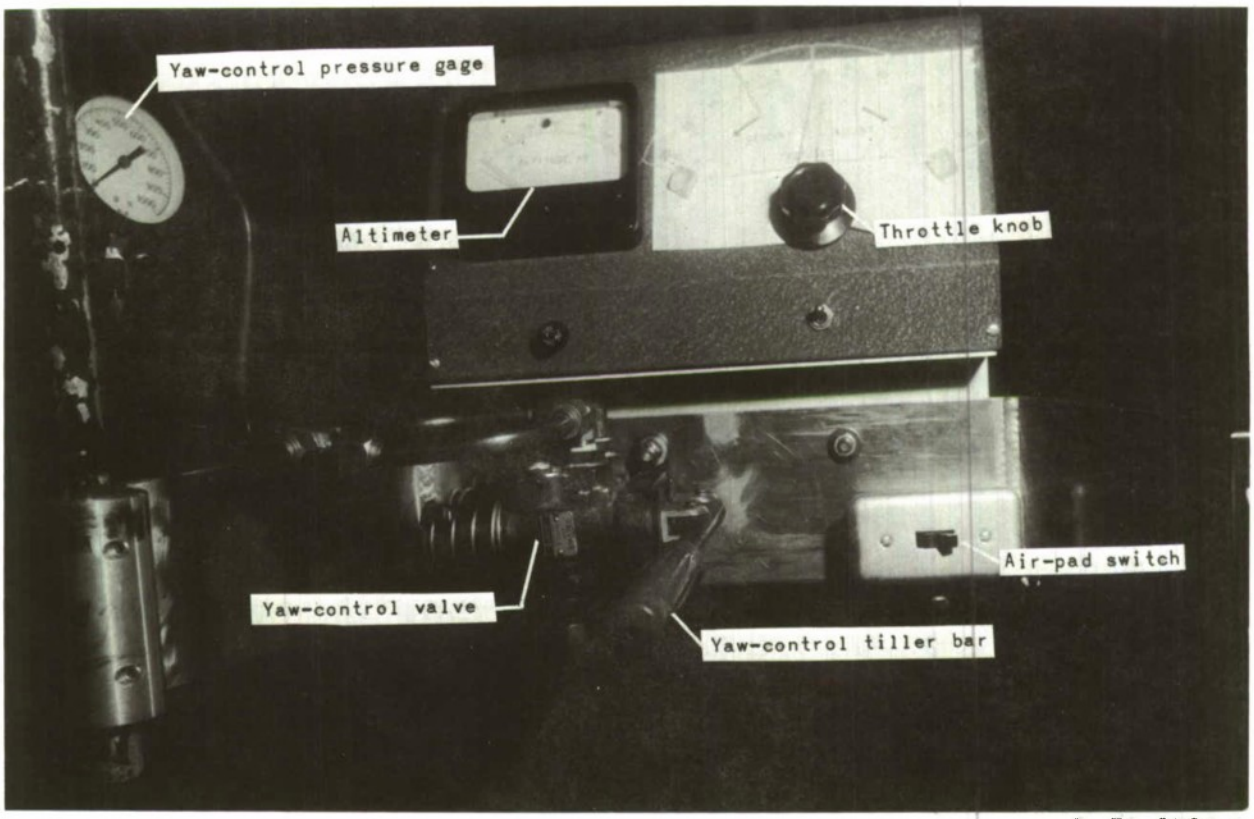

L-70-2720.1

Figure 8.- Control panel.

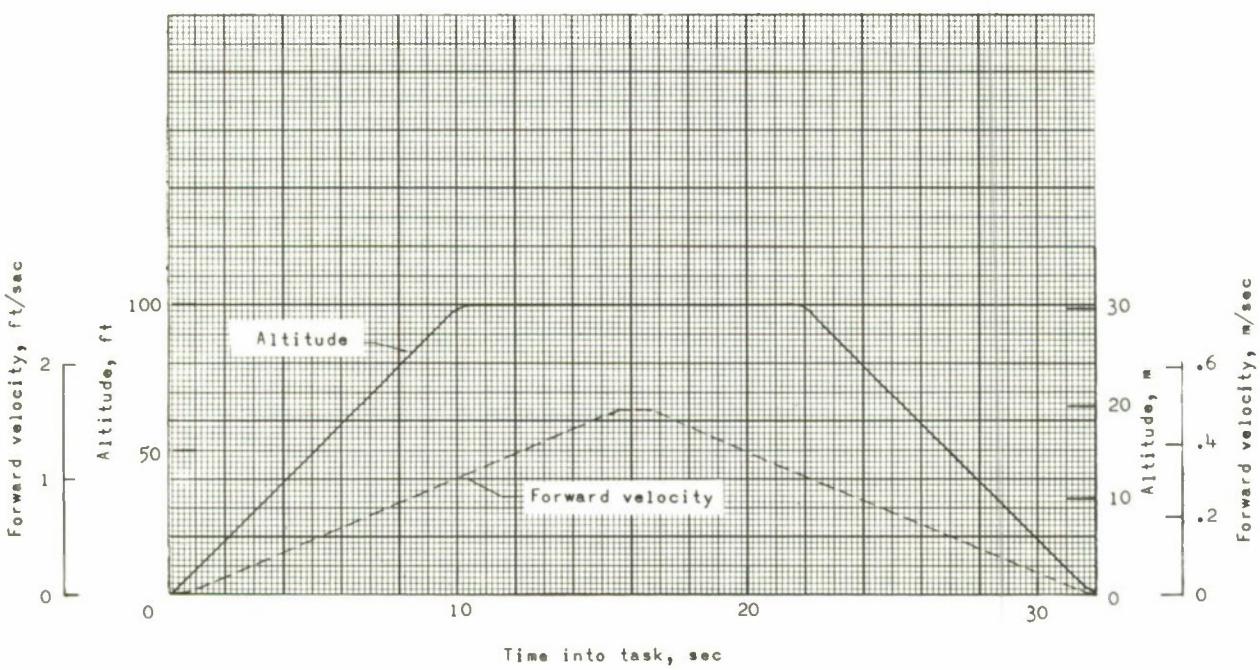

Figure 9.- Typical task profile.

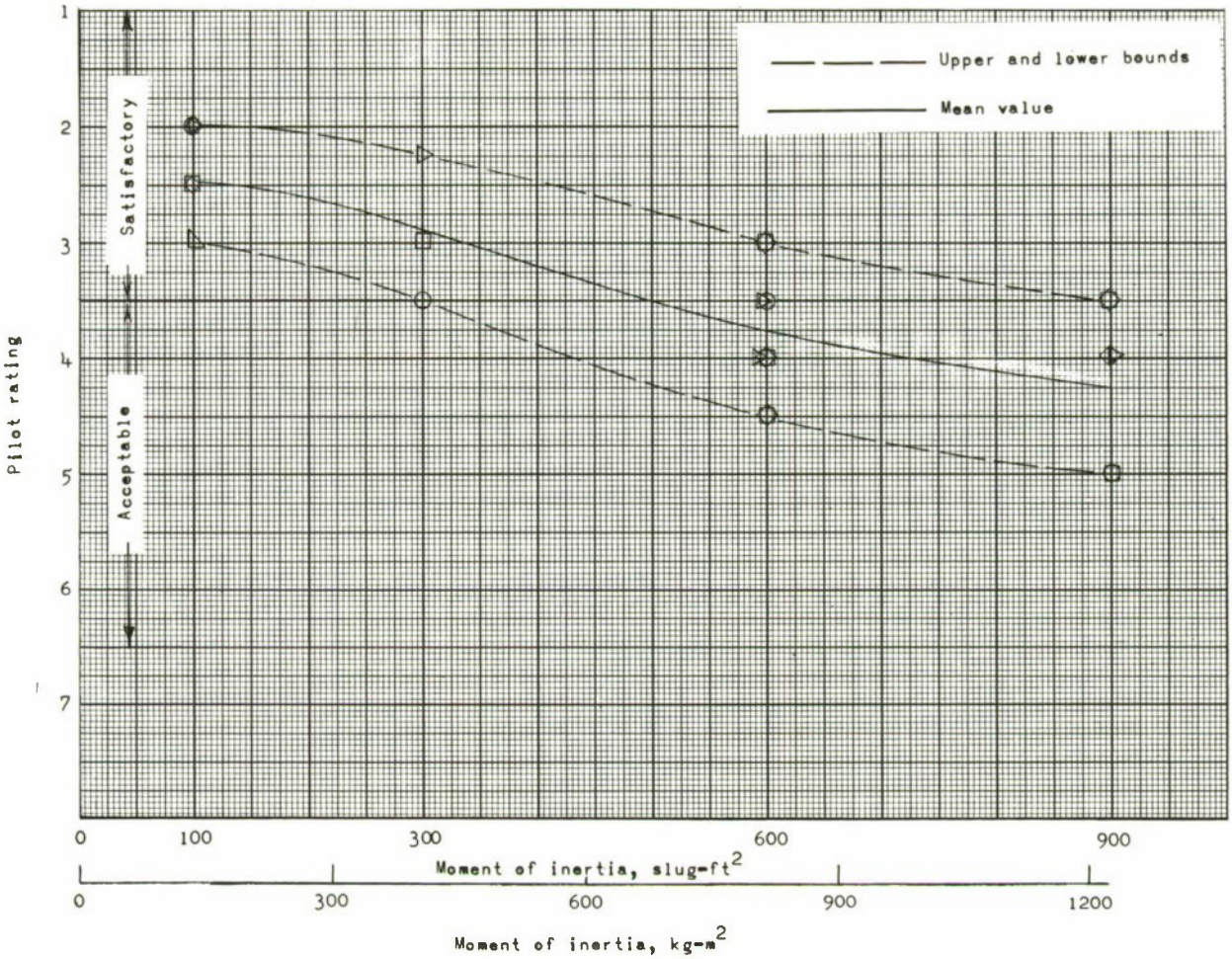

Figure 10.- The effect of inertia on basic configuration.

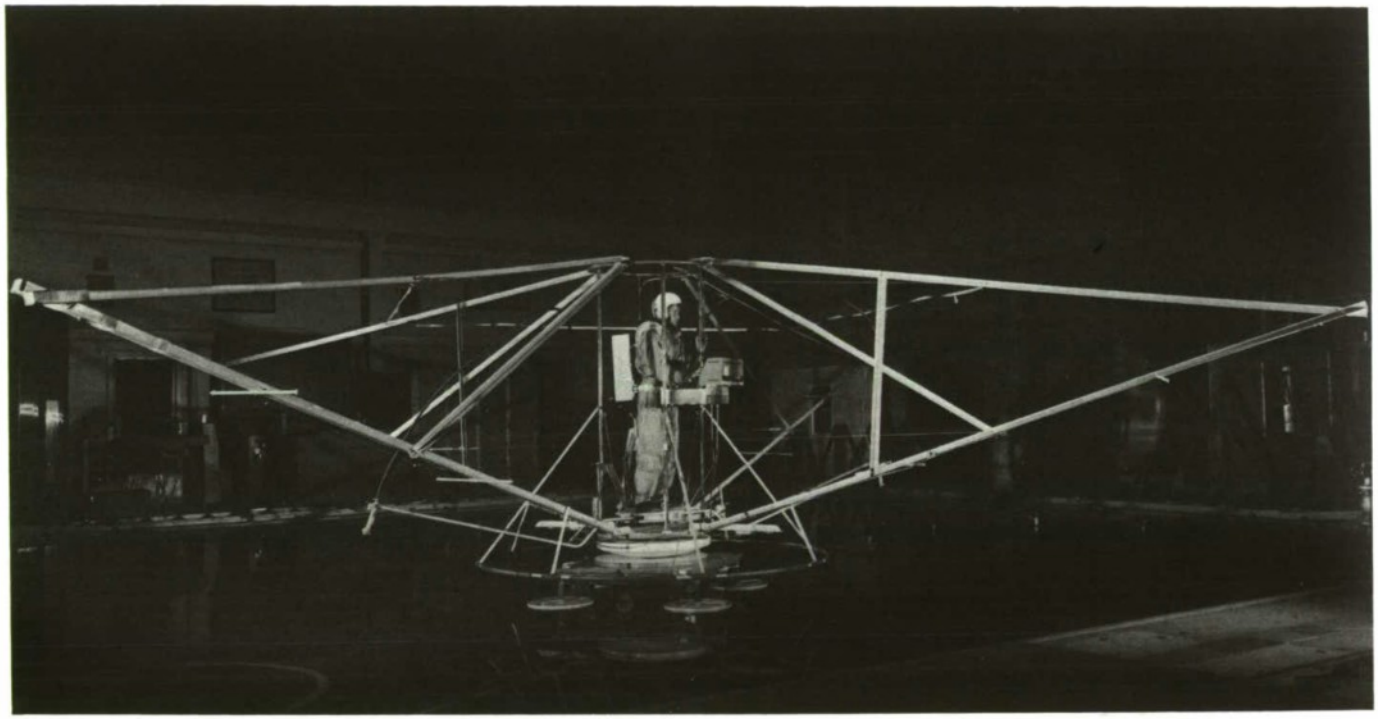

L-70-4395

Figure 11.- Backpack configuration.

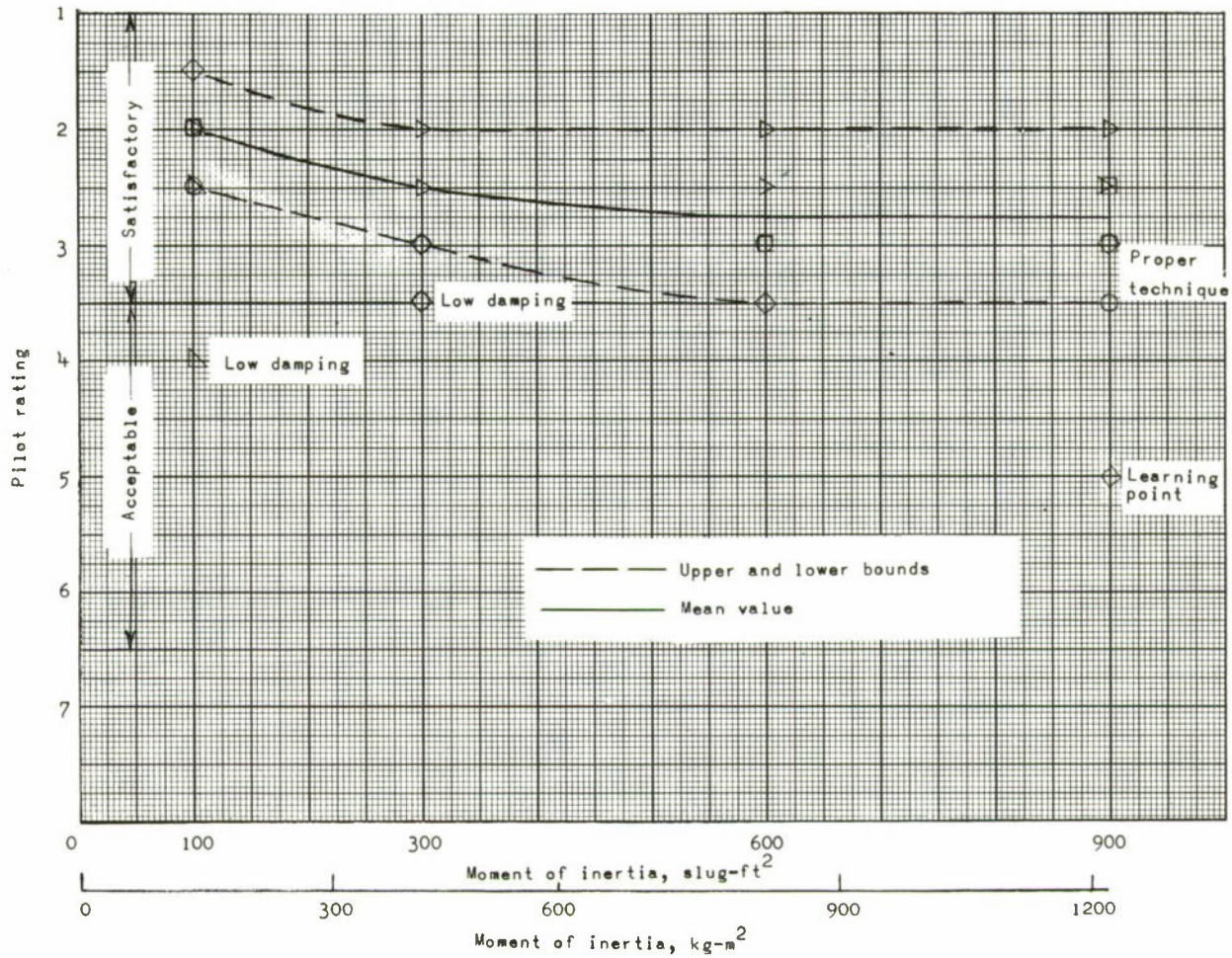

Figure 12.- Auxiliary platform ratings.

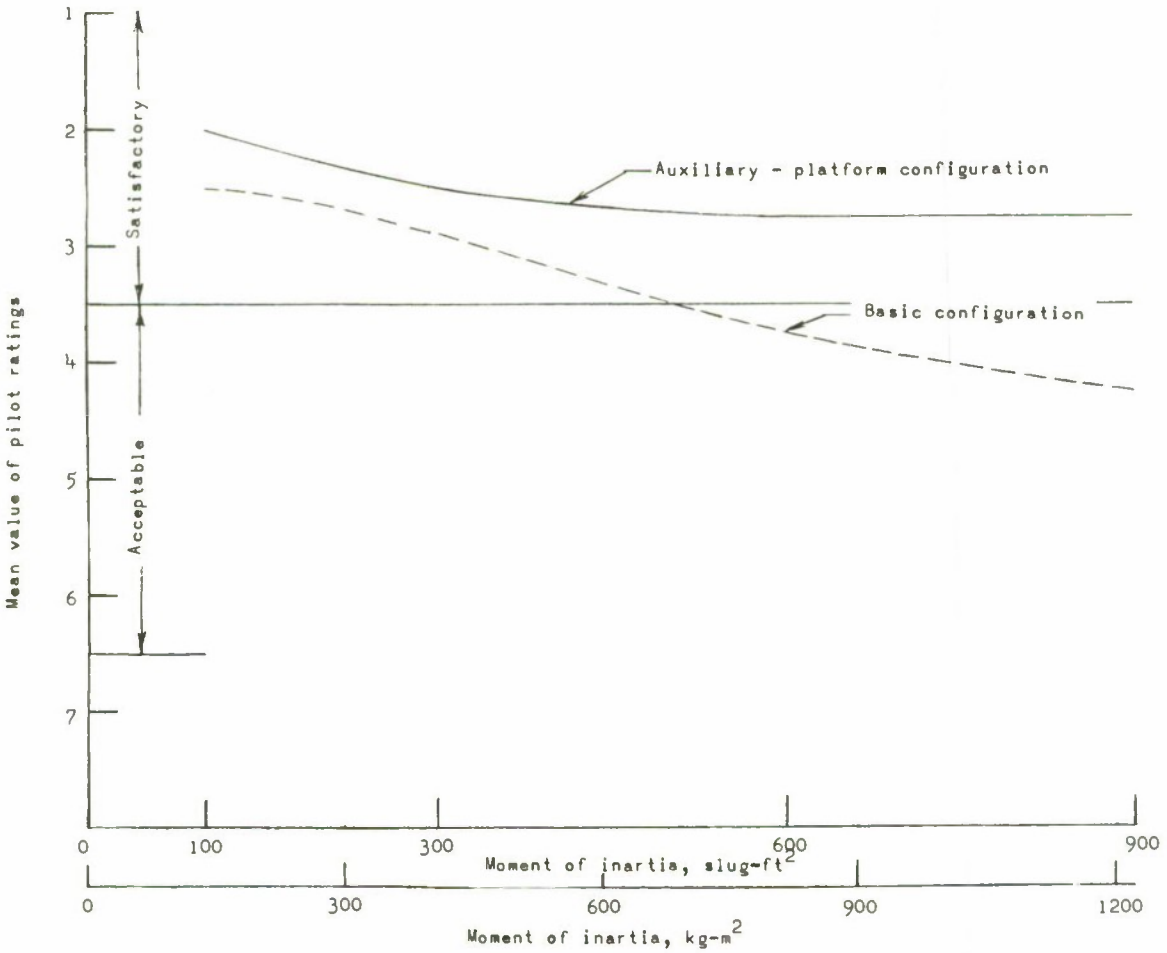

Figure 13.- Comparison of auxiliary-platform and basic-configuration ratings.

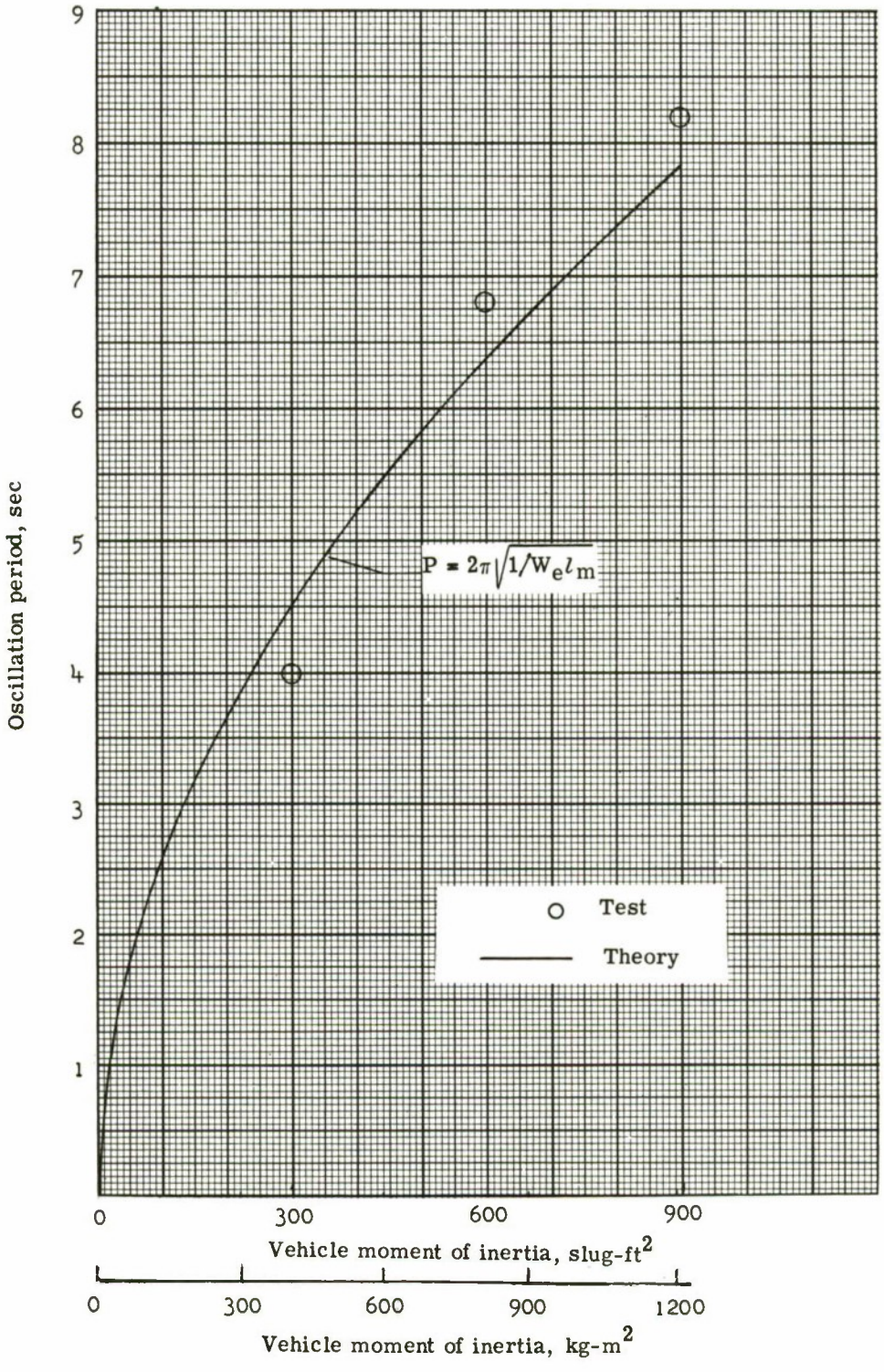

Figure 14.- Vehicle oscillation period.

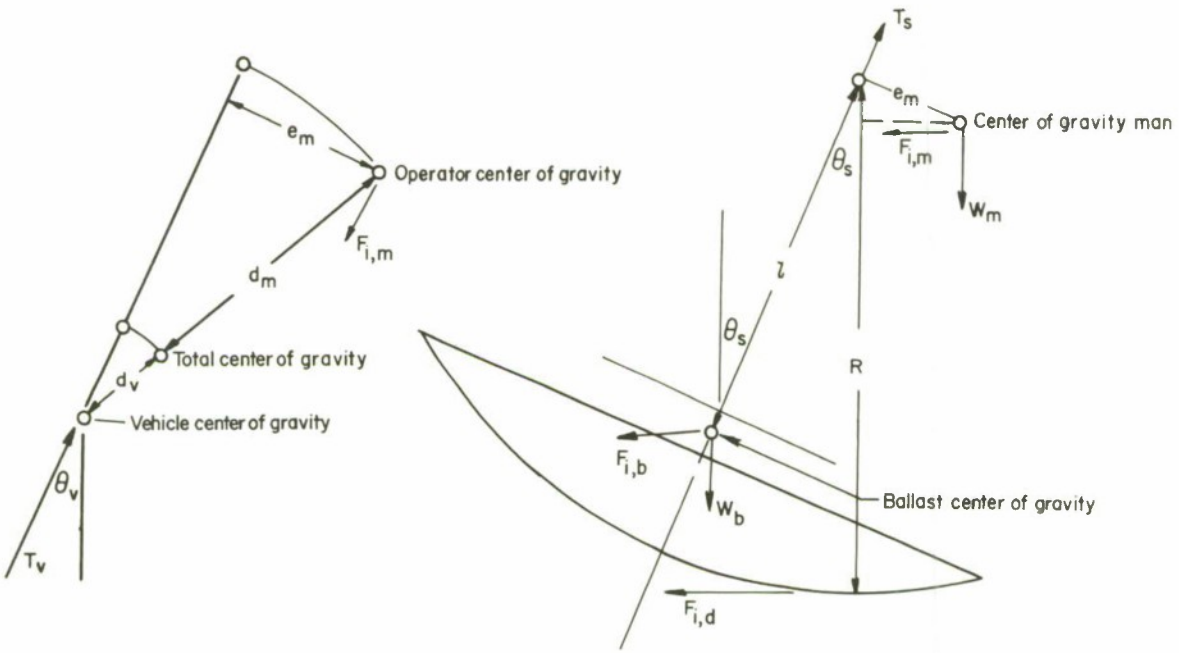

(a) Lunar vehicle. (b) Simulator.

Figure 15.- Basic configurations.

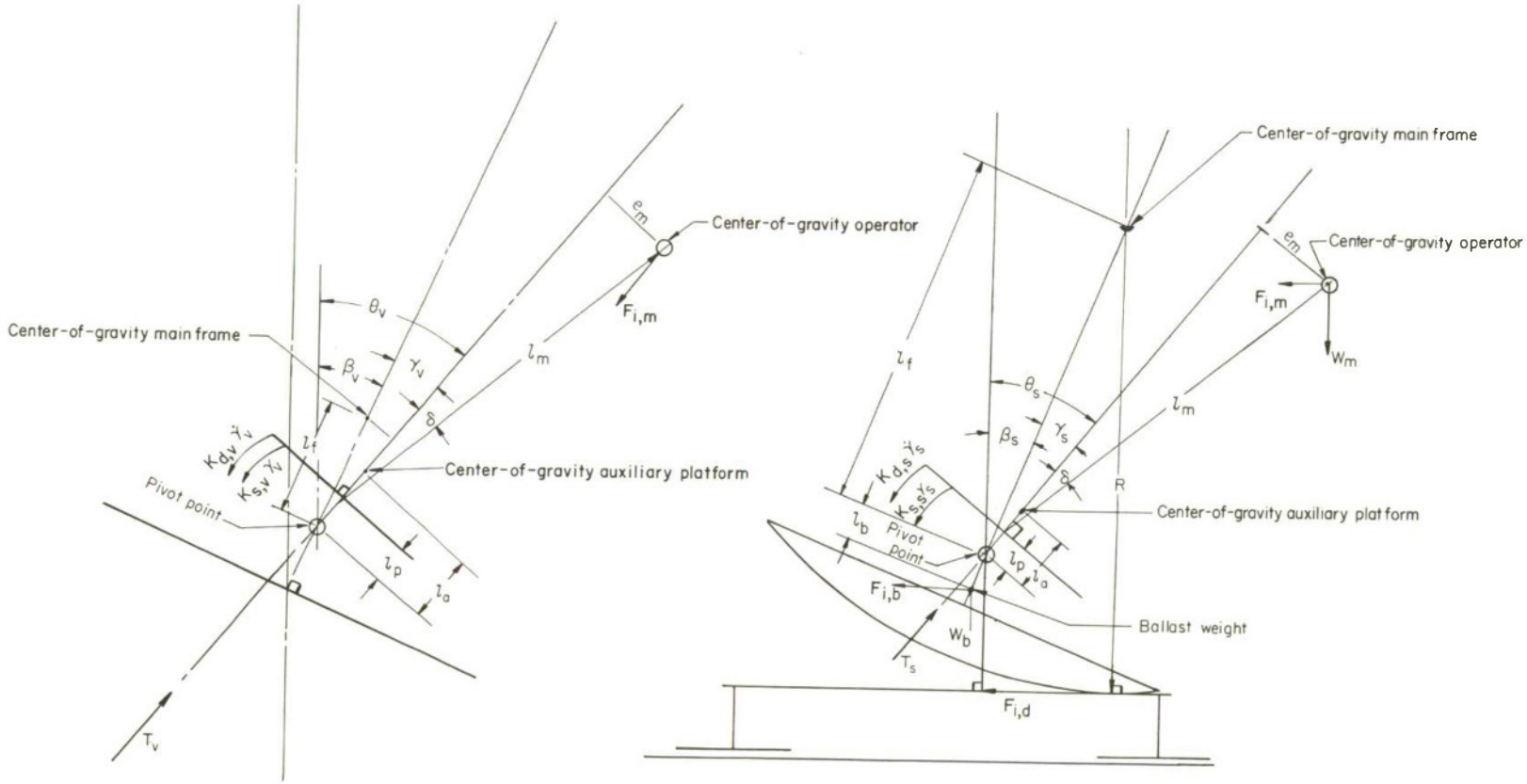

(a) Lunar flying platform.

(b) Simulator.

Figure 16.- Forces acting on an auxiliary platform configuration.

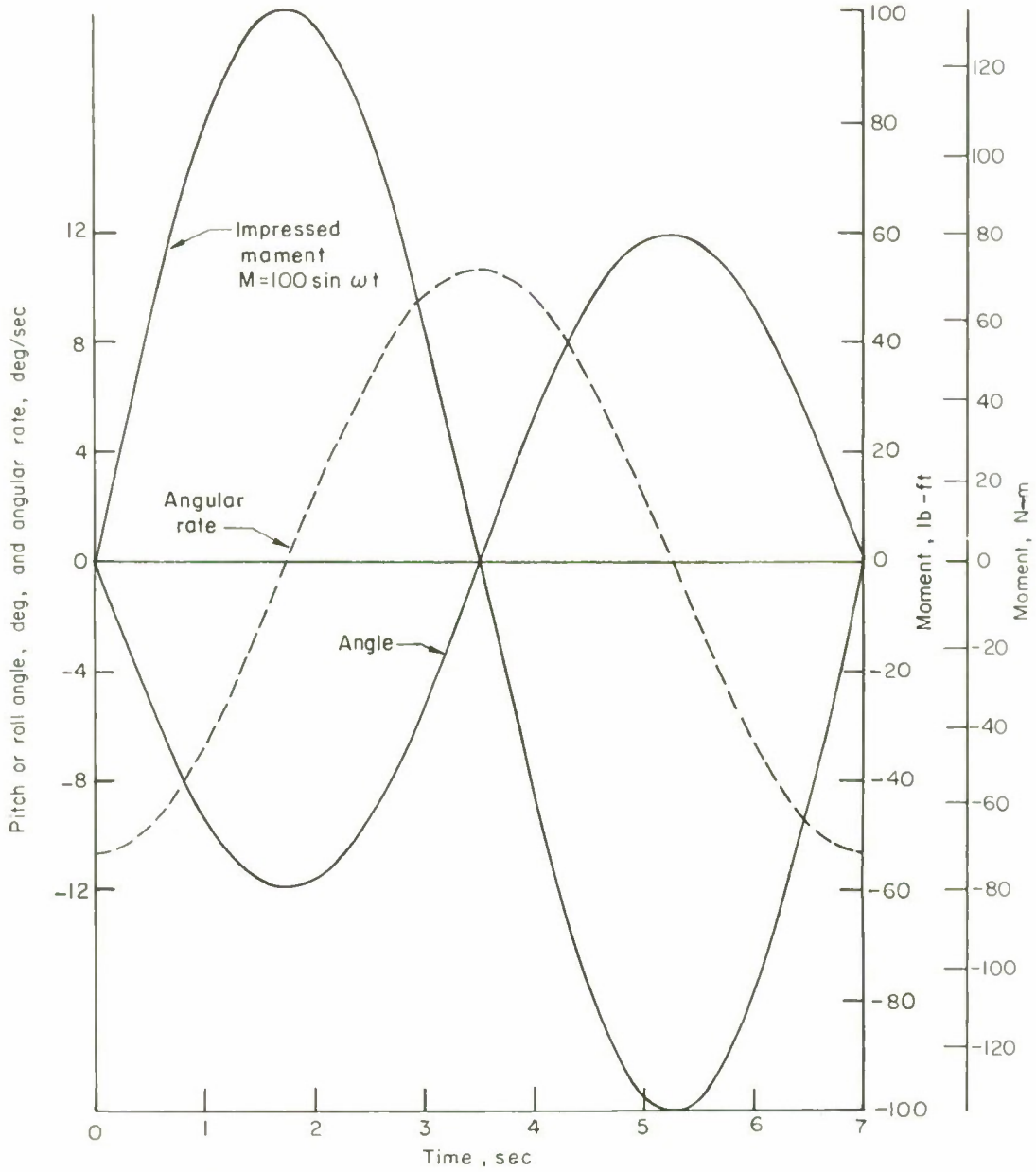

(a) Input moment, angular rate, and attitude.

Figure 17.- Characteristic forced vehicle oscillation. 7-second period; $I = 600$ slug-ft^2 (813 kg-m^2).

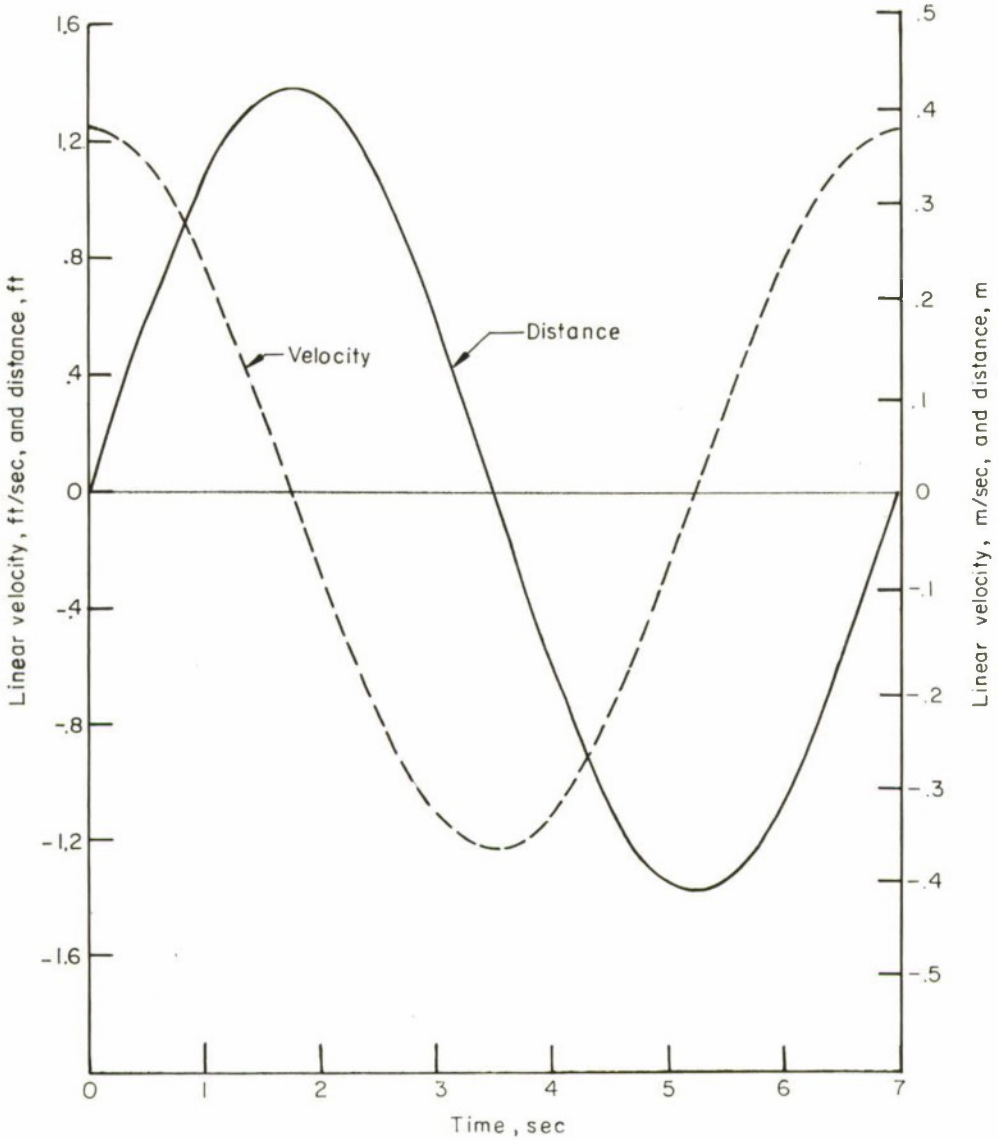

(b) Oscillatory velocity and distance.

Figure 17.- Concluded.

NASA-Langley, 1970 — 11 L-7304

"The aeronautical and space activities of the United States shall be conducted so as to contribute . . . to the expansion of human knowledge of phenomena in the atmosphere and space. The Administration shall provide for the widest practicable and appropriate dissemination of information concerning its activities and the results thereof."

—NATIONAL AERONAUTICS AND SPACE ACT OF 1958

NASA SCIENTIFIC AND TECHNICAL PUBLICATIONS

TECHNICAL REPORTS: Scientific and technical information considered important, complete, and a lasting contribution to existing knowledge.

TECHNICAL NOTES: Information less broad in scope but nevertheless of importance as a contribution to existing knowledge.

TECHNICAL MEMORANDUMS: Information receiving limited distribution because of preliminary data, security classification, or other reasons.

CONTRACTOR REPORTS: Scientific and technical information generated under a NASA contract or grant and considered an important contribution to existing knowledge.

TECHNICAL TRANSLATIONS: Information published in a foreign language considered to merit NASA distribution in English.

SPECIAL PUBLICATIONS: Information derived from or of value to NASA activities. Publications include conference proceedings, monographs, data compilations, handbooks, sourcebooks, and special bibliographies.

TECHNOLOGY UTILIZATION PUBLICATIONS: Information on technology used by NASA that may be of particular interest in commercial and other non-aerospace applications. Publications include Tech Briefs, Technology Utilization Reports and Notes, and Technology Surveys.

Details on the availability of these publications may be obtained from:

SCIENTIFIC AND TECHNICAL INFORMATION DIVISION

NATIONAL AERONAUTICS AND SPACE ADMINISTRATION

Washington, D.C. 20546